universität wien

DIPLOMARBEIT / DIPLOMA THESIS

Titel der Diplomarbeit / Title of the Diploma Thesis

„Evaluation of reporter constructs for Wnt, Notch and Hedgehog pathways“

verfasst von / submitted by

Katarina Peric

angestrebter akademischer Grad / in partial fulfilment of the requirements for the degree of

Magistra der Pharmazie (Mag.pharm.)

Wien, 2019 / Vienna, 2019

Studienkennzahl lt. Studienblatt / degree programme code as it appears on the student record sheet:	A 449
Studienrichtung lt. Studienblatt / degree programme as it appears on the student record sheet:	Diplomstudium Pharmazie
Betreut von / Supervisor:	Univ.-Prof. Dipl.-Ing. Dr. Manfred Ogris
Mitbetreut von / Co-Supervisor:	Dr. Haider Sami

First of all, I want to thank Prof Ogris for giving me the opportunity to be part of his team in the Macromolecular Cancer Therapeutics Laboratory- not only that I've got an insight into the scientific world but I've also spent a lot of joyful moments with all the other members.

Special thanks to Dr. Haider Sami for always having an open door to listen to diploma students and to give advice when needed the most.

In particular, I want to thank Julia Maier who was my great mentor during my time at MMCT Lab. Thank you for teaching me, guiding me and sharing with me your knowledge and your view of science and life itself.

◈◈◈

I also want to thank my dear family who backed me up during my pharmacy studies. Thank you for your encouragement, for your endless support and guidance throughout life!

Table of Contents

1 Introduction

Despite advances in development of antineoplastic therapy in the past decade, cancer as the second largest cause of death remains one of global health issues (Eurostat, WHO 2018). On global level, 1 out of 6 deaths is caused by cancer (WHO, 2018). In 2015. a quarter (25.4%) of total number of deaths in European Union was caused by cancer (Eurostat database). These statistics highlight the importance of cancer research and the need to better understand the process of oncogenesis. The transformation of a healthy cell into a malignant one is still poorly understood. However, deeper insight into the process of oncogenesis leads to development of new anti-cancer treatment strategies for one of today`s most feared diseases.

1.1 Hallmarks of cancer and cancer stem cell model

Oncogenesis, the transformation of normal cells into cancer cells, is a multistep process associated with genetic alterations (Hanahan und Weinberg 2000). Hanahan and Weinberg propose that six crucial alterations in cell physiology are acquired in the process of oncogenesis (Hanahan und Weinberg 2000):

1. Self-dependency on growth signals: reduced dependency on growth signals from microenvironment
2. Insensitivity to antiproliferative signals: as such, cancer cells become “immortal” and able to grow
3. Resistance of programmed cell death: cells are able to acquire activated oncogenes or defects are but are not eliminated through apoptosis
4. Unlimited replication potential: the intrinsic, cell-autonomous program limiting replication is disturbed
5. Induction of angiogenesis: cancer cells are able to induce and sustain angiogenesis
6. Colonization of distant tissue: cancer cells can “move” through the bloodstream and invade distant tissues forming metastases (Hanahan und Weinberg 2000)

These six acquired capabilities are also referred to as “hallmarks of cancer” (Hanahan und Weinberg 2000). Notably, these capabilities are acquired via different mechanisms in distinct types of tumour and at diverse timepoints (Hanahan und Weinberg 2011). In 2011. Hanahan and Weinberg described two additional characteristics which enable malignant growth, referred to as “Emerging hallmarks of cancer”:

- Deregulation of cellular metabolism: cancer cells reprogram energy metabolism to boost cell growth
- Escape from immune destruction: cancer cells avoid detection by the immune system (Hanahan und Weinberg 2011).

Although “hallmarks of cancer” represent acquired features shared by all types of cancer cells, heterogeneity does not appear only in different tumour types but also within distinct cells of a tumour (Dick 2008). Tumours comprise multiple tumour genomes which give rise to various subclones evolving in parallel during the course of tumorigenesis (Kreso und Dick 2014). Proliferating

cells as well as fully differentiated cells form the bulk of a tumour (Clevers 2011). However, neither of them has the ability of self-renewal crucial for tumour development and maintenance (Clevers 2011).

Two general models have been established to explain tumour heterogeneity (Reya et al. 2001). The Cancer Stem Cell Concept (CSC) postulates that only a rare subpopulation within a tumour named "cancer stem cells" or "tumour-initiating cells" is responsible for tumour initiation, growth, metastasis and drug resistance (Chen et al. 2013). Asymmetric division of cancer stem cells leads to heterogeneity and hierarchy between all cells of a tumour (Chen et al. 2013).

Cancer stem cells are defined by following characteristics (Ward und Dirks 2007):

- self-renewal: cancer stem cells are able to self-renew if transplanted *in vivo*
- tumour initiation: injected *in vivo*, cancer stem cells are able to regenerate the tumour from which they were derived
- differentiative capacity: tumours which arise *in vivo* should be phenotypically equal to the original tumour

By contrast, the stochastic model, also referred to as clonal evolution model, postulates that all cells are equipotent within a tumour and thus able to regenerate a tumour and maintain its growth *in vivo* (Ward und Dirks 2007; Karamboulas und Ailles 2013). According to this model, every cell can potentially give rise to new tumours (Karamboulas und Ailles 2013). Neither of the two models can be considered as the right one, rather both concepts can be used to describe tumour heterogeneity (Karamboulas und Ailles 2013).

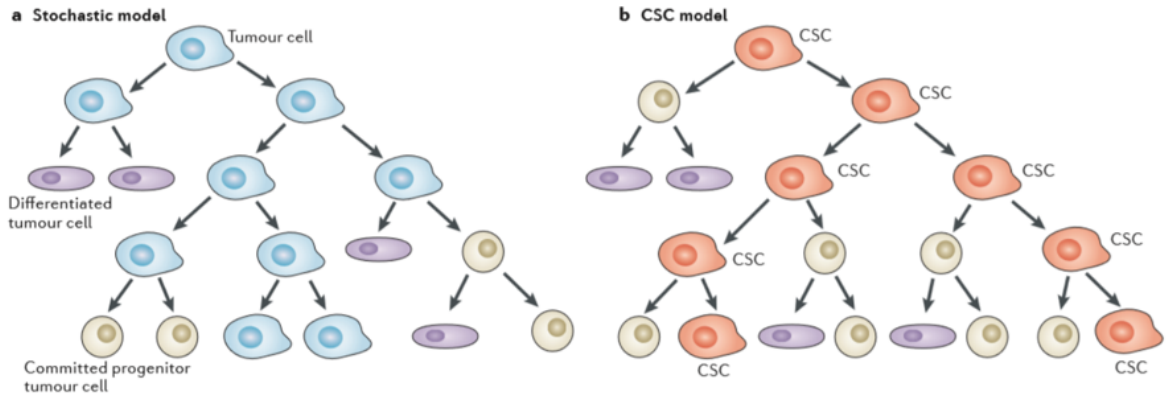

Figure 1. Two distinct models of tumour growth: a) In the stochastic model, all cells are equipotent. Every cell is able to self-renew, to differentiate and give rise to a new tumour. Some tumour cells divide clonally whereas others differentiate, resulting in heterogeneity. b) In the cancer stem cell (CSC) model, only a subpopulation of tumour cells has the capability of long-term self-renewal and is thus able to give rise to a new tumour. Cancer stem cells divide asymmetrically resulting in an identical cancer stem cell with self-renewal ability and in a more differentiated cell (figure from Beck and Blanpain 2013)

However, if the Cancer Stem Cell (CSC) model was correct, eradication of cancer stem cells from a tumour would stop tumour growth (Nguyen et al. 2012). Hence, it would be desirable to separate cancer stem cells from other tumour cells. In general, cancer stem cells are distinguishable from other tumour cells through distinct and specific biomarker phenotypes such as cell surface markers (Chen et al. 2013). Cell surface markers also expressed in non-malignant-cells (Al-Hajj et al. 2003), allow sorting of marker-positive and marker-negative subpopulations of cancer cells (Clevers 2011). Since Al-Hajj et al. successfully isolated cancer stem cells from breast cancer by using the CD24 and CD44 marker combination, cancer stem cells were also identified in other solid tumours (Tirino et al. 2013). Fluorescence activated cell sorting (FACS) is a method which enables separation and identification of marker-positive and marker-negative cells (Clevers 2011). In our work, FACS was used for sorting of cancer cells with the focus set on developmental signalling pathways which are typically deregulated in many tumour types.

1.2 Nucleic acid delivery in gene therapy

Gene therapy uses vehicles or vectors to therapeutically deliver genes of interest into cells of a patient`s body in order to treat inherited (e.g. single gene disorders) or acquired (e.g. cancer) diseases (Jin et al. 2014; Chira et al. 2015). The intention is to compensate for gene deficiencies or to provoke gene silencing of pathogenic genes (Cengizeroglu 2012).
Vectors for gene delivery can be either viral or non-viral (Chira et al. 2015). Initially, the focus was on development of viral vectors due to their natural ability of cell-specific transduction and relative high transfection efficiency (Jin et al. 2014). However, viral vectors can have certain disadvantages in contrast to non-viral vectors, such as poorer biosafety (e.g. unexpected immune host response), limited loading capacity, difficulties in handling and large-scale production (Cengizeroglu 2012; Jin et al. 2014). In addition, viral vectors bear the risk of endogenous virus recombination which can eventually lead to oncogenic deregulation (Niidome und Huang 2002; Cengizeroglu 2012). For this reason, synthetic delivery systems have been extensively developed in the past two decades.
Such synthetic derived vectors are easy to handle and allow inexpensive production on large scale (Chira et al. 2015). Most importantly, they have clear advantages regarding biosafety and biodegradability (Chira et al. 2015).

In general, non-viral gene delivery systems can be divided into two categories: Physical methods such as electroporation, gene gun, ultrasound or hydrodynamic injection utilize pressure or electricity to deliver nucleic acids into cells (Niidome und Huang 2002). Synthetic carriers comprise cationic polymers (e.g. PEI), cationic lipids (e.g. DOTAP) or cationic polysaccharides (e.g. Chitosan) (Wolff und Rozema 2008). These carriers interact with nucleic acid based on a simple principle: Cationic lipids or polymers condense negatively charged nucleic acid by electrostatic interaction forming nano-sized complexes called “lipoplexes” or “polyplexes” (Wolff und Rozema 2008; Zhang et al. 2012; Jin et al. 2014).

The following section provides more detailed information about biochemical characteristics of linear polyethylenimine (LPEI) which was used as transfection reagent in our experiments.

1.2.1 Linear polyethylenimine as transfection reagent

Polyethylenimine is an organic polymer consisting of repeating units of ethylenimine (https://en.wikipedia.org/wiki/Polyethylenimine). Hence, every third atom is a nitrogen within an amine group, which can be protonated featuring it with excellent buffering capacity within a broad pH range (Boussif et al. 1995a). Two forms of polyethylenimine exist: linear polyethylenimine (LPEI) and branched polyethylenimine (BPEI) (Neu et al. 2005).

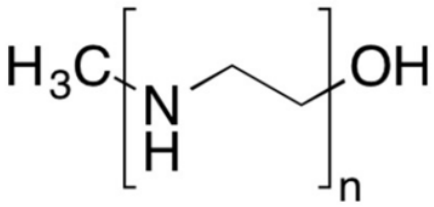

Figure 5. Linear polyethylenimine (LPEI): LPEI is a branched polymer consisting of repeating units of protonable nitrogen (secondary amine groups) and aliphatic carbon ions (ethyl groups) (Wikipedia; figure from polysciences)

Wightman et al revealed in their experiments that linear polyethylenimine has a higher transfection efficiency *in vitro* compared to branched polyethylenimine when polyplexes were generated in salt containing buffer (Wightman et al. 2001).
As a general rule, transfection efficiency and biophysical properties such as size and charge depend mainly on two parameters: molecular weight of the polycation and nitrogen to phosphate ratio (Choosakoonkriang et al. 2003; Vu et al. 2012)

Molecular weight: Polyethylenimine in the range of 5-25 kDa is generally most convenient for gene delivery (Neu et al. 2005). Low molecular PEI has relatively low cytotoxicity and releases its cargo easily. However, it is less efficient regarding condensation of plasmid DNA (pDNA) compared to high molecular PEI (Neu et al. 2005). The latter, however, has a greater ability to condense pDNA but performs worse regarding cargo release and cytotoxicity (Jin et al. 2014). In addition, high molecular PEI has poorer biodegradability as it lacks biodegradable bonds as it contains almost exclusively C-C or C-N bonds (Moghimi et al. 2005; Kawakami et al. 2006).

Nitrogen to phosphate ratio: N/P ratio is defined as molar ratio of phosphate in the nucleic acid and nitrogen in polyethylenimine (Boeckle et al. 2004). To increase gene delivery and thus transfection efficiency, polyplexes of higher N/P ratios should be prepared ((Boeckle et al. 2004). In general, polyplexes at N/P ≤3 are neutral and tend to aggregate, whereas polyplexes prepared at higher N/P ratio are small and positively charged (Kircheis und Wagner 2000; Boeckle et al. 2004). Polyplexes with N/P ratio ≥3 have an excess of free PEI which promotes endosomal escape and transfection efficiency (Boeckle et al. 2004; Jin et al. 2014). However, free PEI increases cytotoxicity (Zhang et al. 2012).

Gradinetti et al reported that LPEI based DNA polyplexes provoke depolarization of mitochondrial membranes inside cells (Grandinetti et al. 2011; Zhang et al. 2012). As a general rule, polycations interact in a non-specific manner with anionic mitochondrial and cytoplasmic membranes (Miyata et al. 2012). PEI based polyplexes administered *in vivo* may interact with blood components such as erythrocytes. Hence, aggregation in lung capillaries and eventually lung embolism may be provoked (Ogris et al. 1998; Kircheis und Wagner 2000; Wightman et al. 2001). Thereby, the right balance between high transfection efficiency and low cytotoxicity has to be found (Jin et al. 2014).

In our transfection experiments, LPEI with an average molecular weight of 10kDa was used which was synthesized in our lab by Alexander Taschauer according to Roedl et al. (Rödl et al. 2013). All polyplexes were generated at N/P 9 as Islam Abd El Rahman received better results regarding transfection efficiency of A549 cells with N/P 9 than N/P 6 (Abd El Rahman 2017).

1.2.2 Intracellular gene delivery of polyplexes

In order to be internalized by cells, polyplexes associate to the cell membrane and enter through endocytosis (Miyata et al. 2012). It has been commonly assumed that endocytosis occurs within 4 hours after transfection (Rémy-Kristensen et al. 2001; Miyata et al. 2012). Uptake via endocytosis is possible due to electrostatic interaction between positively charged PEI from polyplexes and negatively charged proteoglycans of the cell membrane (Kircheis und Wagner 2000). Once inside the cell, polyplexes have to escape from endosomal vesicle and thus lysosomal degradation as endosome matures to lysosome (Wolff und Rozema 2008). The pH decrease from extracellular neutral (7.4), to early endosomal (6.5) and finally late endosomal acidic (5.5) is crucial for endosomal escape of polyplexes (Miyata et al. 2012). The generally most accepted explanation for endosomal escape is the “proton sponge hypothesis” postulated by Behr in 1994 (Di Gioia und Conese 2009):
Amine groups of PEI are protonated at acidic condition of the endosome leading to an influx of chloride as counterions (Miyata et al. 2012). Water is subsequently absorbed from the cytosol resulting in high osmotic pressure (Funhoff et al. 2004). Osmotic swelling of the endosome eventually induces endosomal disruption and thus endosomal escape of the polyplexes (Boussif et al. 1995b; Di Gioia und Conese 2009; Miyata et al. 2012).

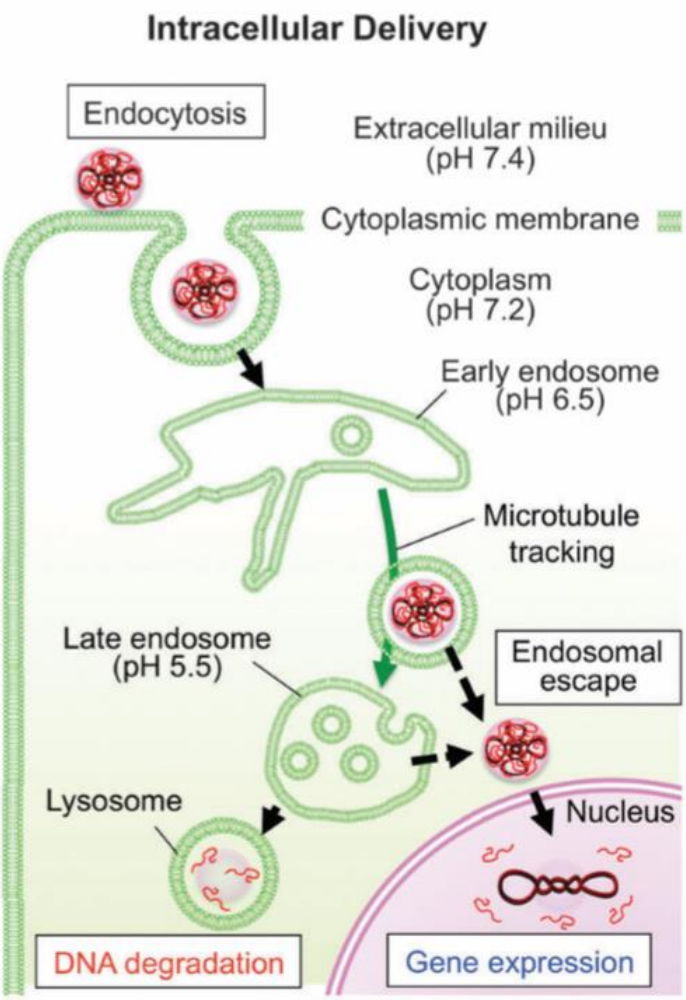

Figure 6. Intracellular gene delivery of polyplexes: Polyplexes enter the cell by endocytosis due to electrostatic interaction with the cell membrane. Inside the cell, polyplexes have to escape from endosomal vesicle to avoid lysosomal degradation. Due to pH decrease from neutral (7,4) to acidic (5,5), polyplexes are able to escape the endosome through the "proton sponge effect". Once released, polyplexes enter the nucleus and trigger gene expression. (figure from Miyata et al.)

Once released, polyplexes must reach the perinuclear region and enter the nucleus in order to trigger gene expression (Neu et al. 2005). To date, it is still unclear at which point polyplexes release their DNA payload and through which mechanism nucleic acid reaches the nucleus (Neu et al. 2005; Di Gioia und Conese 2009).The nuclear membrane is perforated with nuclear pore complexes (NPC) allowing macromolecules with size of ≤50 kDa to diffuse freely (Talcott und Moore 1999; Di Gioia und Conese 2009). Polyplexes, however, have an average size of 100-200 nm in buffer solution which makes entrance via nuclear pores difficult (Miyata et al. 2012). For that reason it is believed that plasmid DNA, whether free or still complexed with PEI, is imported passively into the nucleus during mitosis accompanied by disintegration of nuclear membrane (Di Gioia und Conese 2009; Miyata et al. 2012).

1.3 Reporter gene constructs for visualization of pathway activity

Developmental signalling pathways influence regulation of gene expression in cells by promoting interaction of transcription factors with responsive elements in the promoter regions of target genes (Naylor 1999). In order to understand how deregulated signalling pathways affect gene transcription, reporter gene constructs can be used (Naylor 1999). Reporter gene constructs contain relevant promoter elements being activated by the signalling pathways of interest. They drive the expression of the reporter gene encoding for reporter proteins (Naylor 1999). Among reporter proteins, fluorescent proteins and luciferases are widely used to visualize transgene expression level and promoter activity (Youn und Chung 2013). Transcriptional activity of reporter proteins then directly correlates with transcriptional activity of genes of interest (e.g. by using similar promoter elements). Hence, reporter gene expression provides indirect information about activity of pathway-dependent promoters (Youn und Chung 2013). In this way, activity of signalling pathways can be visualized.

Reporter construct 3P-TOP

The major goal of this thesis was to assess the functionality of a fluorescent reporter gene construct called 3P-TOP cloned with the aim to visualize activity of Wnt, Notch and Hedgehog pathways. The reporter construct (figure 7) consists of a MuLE backbone and three pathway-specific promoters (CBF, TOPFlash, hPTCH1) which are fused to reporter genes encoding fluorescent proteins (tdTomato, iRFP, mTurquoise2). Furthermore, 3P-TOP contains constitutive active cytomegalovirus (CMV) promoter attached to enhanced green fluorescent protein (EGFP). Due to constitutive promoter activity, EGFP is always expressed independent from Wnt, Notch or Hedgehog pathway activity. EGFP provides information about transfection efficiency as it is expressed in every successfully transfected cell.

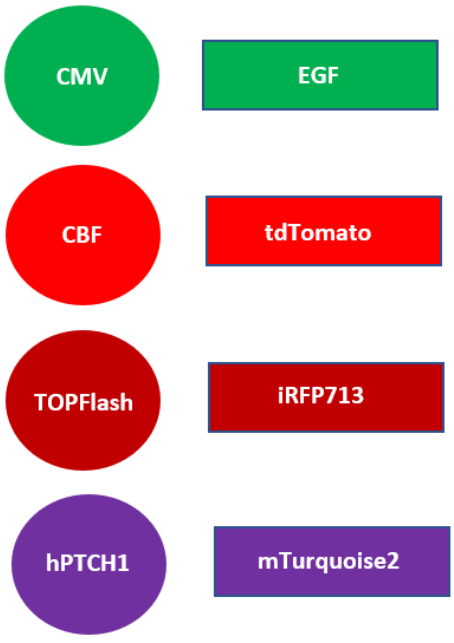

Figure 7. 3P-TOP: Reporter construct 3P-TOP comprises one constitutive active (CMV) and three pathway-dependent promoters (CBF, TOPFlash, hPTCH1) fused to fluorophores (EGFP, tdTomato, iRFP713, mTurquoise2)

Besides testing of our reporter construct 3P-TOP, each pathway-dependent promoter was tested for its inducibility and pathway-specificity. Promoter activity was induced upon addition of pathway-specific activators and compared to inducibility of the respective mutated version (CBFREMut, FOPFlash, hPTCHMut). The next section describes pathway-dependent promoters and activators which were used in our experiments:

Promoters and activators of the Notch pathway

- CBF and CBFREMut were used. The CBF promoter binds to transcription factor CBF1 which interacts with NICD (Notch intracellular domain) and drives expression of Notch target

genes (Nowotschin et al. 2013). CBFREMut is the mutated version of CBF1 responsive element (Mizutani et al. 2007). It was used as negative control as it is less efficient regarding transcriptional activity.

- Pathway-specific activators: Human EFhICN1 (cloned from EFhICN1.CMV.eGFP; Addgene plasmid # 17623) and murine pCAGGS-NICD (Addgene plasmid # 26891) were used to activate Notch signalling pathway. Both plasmids encode the intracellular domain of the Notch receptor (NICD) which binds to transcription factor CBF1. In our experiments, EFh-ICN1 and pCAGGS-NICD were co-transfected with CBF and CBFREMut promoters to induce their activity.

Promoters and activators of the Wnt pathway

- TOPFlash, FOPFlash and CTP4 were used. TOPFlash is a β-catenin/TCF dependent Notch promoter which contains multiple binding sites for TCF responsive element (Chtarbova et al. 2002). FOPFlash comprises mutated binding sites for the transcription factor and was used as negative control (Korinek 1997; da Costa et al. 1999).
- CTP4 is a synthetic β-catenin/TCF dependent promoter developed by Lipinsky et al. It contains ten TCF binding sites and E1B TATA box which increases β-catenin dependency (Lipinski et al. 2004). In our experiments, CBF and CTP4 were compared for their Wnt-dependency. A mutated version of CTP4 promoter is not available.

- Pathway-specific activators: Human recombinant Wnt3A is a protein which was used for activation of Wnt-dependent promoters (TOPFlash, FOPFlash, CTP4). Encoded by one of the 19 human Wnt genes, Wnt3A is a secreted glycoprotein which acts as a ligand for the Wnt pathway (Willert und Nusse 2012). Binding to the Frizzled Family receptors, Wnt3A activates Wnt signalling cascade resulting in stabilization of β-catenin and consequent expression of Wnt target genes (MacDonald und He 2012).
- LiCl was also used to induce Wnt promoters. Wnt3A and LiCl were compared regarding Wnt pathway-specificity. Stambolic et al observed that Lithium ions inhibit GSK3β leading to stabilization of β-catenin and thus activation of β-catenin/TCF-induced transcription. In this way, Lithium mimics Wnt signalling (Stambolic et al. 1996; Chtarbova et al. 2002).

Promoters and activators of the Hedgehog pathway

- hPTCH1-wt and hPTCHMut were used. hPTCH1-wt contains wild type binding sites for GLI1. GLI1 belongs to GLI zinc finger transcription factors which are mediators of the Hedgehog signalling pathway (Winklmayr et al. 2010). hPTCHMut has mutated binding sites for GLI and was used as a negative control.

- Pathway-specific activators: Recombinant human Sonic Hedgehog (shh) is a protein used to enhance promoter activity of hPTCH1-wt. Through binding to Patched (PTCH) receptor, smoothened (SMO) receptor is no longer repressed by PTCH. Consequently, SMO triggers several intracellular events which leads to activation of the zinc finger transcription factors GLI. Hence, transcription of HH target genes is induced (Tian 2009).

1.3.1 Fluorescent reporter proteins

In Fluorescence reporter gene assays, genes encoding for fluorescent proteins are fused to promoters of interest. In this way, expressed fluorescent protein correlates with transcriptional activity of the promoter. Thus, promoter activity and function can be visualized dynamically inside cells or living tissue (Naylor 1999). Since the discovery of green fluorescent protein (GFP) in bioluminescent jellyfish *Aequorea Victoria* in the 1960s, a large variety of colour-shifted genetic derivatives of GFP has been introduced emitting in the cyan (cyan fluorescent protein, CFP), blue (blue fluorescent protein, BFP) and yellow (yellow fluorescent protein-YFP) range (www.microscopy.com). Fluorescent proteins which emit in the range of longer wavelengths (orange-red) have been developed from other marine organisms such as *Discosoma striata* and *Anthozoa* (www.microscopy.com). The principle behind is that fluorescent proteins are excited at a certain wavelength and emit light of longer wavelengths, which can be detected by e.g. flow cytometry (Choy et al. 2003). Since a large variety of fluorescent proteins is available, the choice of the right fluorophores, especially if used in multi-label experiments, is not easy.
In general, fluorophores should fulfil following requirements:

- High expression efficiency and low cytotoxicity (Shaner et al. 2005)
- High fluorescence intensity (brightness) to be detected above autofluorescence (Shaner et al. 2005)
- Photostability for at least the duration of the experiment (Shaner et al. 2005)
- No or very low interference with other fluorophores in terms of excitation and emission if used in multi-label experiments (Shaner et al. 2005)

In the following section, fluorescent proteins which were used in our experiments are introduced:

- **mTurquoise2:** MTurquoise2 is an enhanced monomeric variant of cyan fluorescent protein (CFP) (Goedhart et al. 2012). mTurquoise2 is excited at a wavelength of 434nm and shows an emission maximum at 474nm (www.fpbase.org). Due to its high quantum yield, it is a brighter variant with improved maturation rate (Goedhart et al. 2012).

- **EGFP**: The Enhanced green fluorescent protein is a monomeric derivative from Green fluorescent Protein (GFP) originally discovered in jellyfish *Aequorea Victoria* (Choy et al. 2003). EGFP is maximally excited at 488nm and maximum emission appears at 507nm (Shaner et al. 2005). Among Aequorea GFP derivatives, EGFP is among the brightest and most photostable fluorescent one (Day und Davidson 2009).

- **Venus**: Venus is one of the brightest yellow fluorescent proteins (YFP) (Day und Davidson 2009). It is maximally excited at 515nm and has an emission peaks at 528nm (Shaner et al. 2005). Generally, Yellow fluorescent proteins (YFP) are sensitive to acidic pH, chloride ions and have poor photostability (Day und Davidson 2009). Nagai and colleagues succeeded in increasing pH stability and maturation efficiency while reducing halide sensitivity which eventually resulted in the derivate Venus (Nagai et al. 2002; Day und Davidson 2009). H2B-Venus is a fusion of human histone H2B and yellow fluorescent protein Venus (Nowotschin et al. 2013) which was used in our experiments. Fluorescent proteins tagged

to histones are bound to chromatin even during cell division. In this way, tracking of a single cell and their progeny is possible (Nowotschin et al. 2013). Venus can behave either as a monomer or as a weak dimer (Shaner et al. 2005).

- **tdTomato**: The tandem dimer tdTomato is a derivative from DsRed, the first coral-derived fluorescent protein obtained from *Discosoma striata* (Day und Davidson 2009). Maximum excitation wavelength is at 554nm and maximum emission wavelength at 581nm (Shaner et al. 2005). TdTomato is a fusion of two copies of tdTomato genes which was created to achieve high brightness and low intracellular aggregation (Campbell et al. 2002; Shaner et al. 2004). In addition, it is one of the most photostable fluorescent proteins (Day und Davidson 2009).

- **iRFP713:** IRFP713 also referred to as iRFP, is a phytochrome-based dimeric near infrared fluorescent protein. IRFP has maximum excitation at 690nm and maximum emission at 713nm. It contains biliverdin as chromophore, which is an intermediate from heme metabolism and thus endogenous to mammalian cells (Filonov et al. 2011; Lecoq und Schnitzer 2011). Since iRFP has excitation and emission spectrum near infrared wavelengths, this allows its analysis also in deep tissue *in vivo* (Lecoq und Schnitzer 2011). Thus, iRFP has high potential for whole-body imaging techniques (Lecoq und Schnitzer 2011).

1.3.2 Fluorescent compensation in multi-colour experiments

Simultaneous detection of multiple fluorescent proteins by flow cytometry enables to differentiate between distinct cell populations or to assess expression and function of multiple genes of interest (Hawley et al. 2004). Our reporter construct 3P-TOP contains genes of four fluorescent proteins, EGFP, tdTomato, iRFP and mTurquoise2 respectively. Although fluorescent proteins were chosen considering mutual excitation and emission spectra, spectral interplay of fluorescence signal is almost inevitable. For proper evaluation by flow cytometry, spectral overlap needs to be corrected with signal compensation.In flow cytometry, fluorescent proteins excited at certain wavelength emit fluorescence passing a bandpass filter which allows only a range of wavelengths to pass through (Tung et al. 2004). Subsequently, the bandpass filter determines which detector will measure fluorescence signal of each fluorescent protein (www.expertcytometry.com).

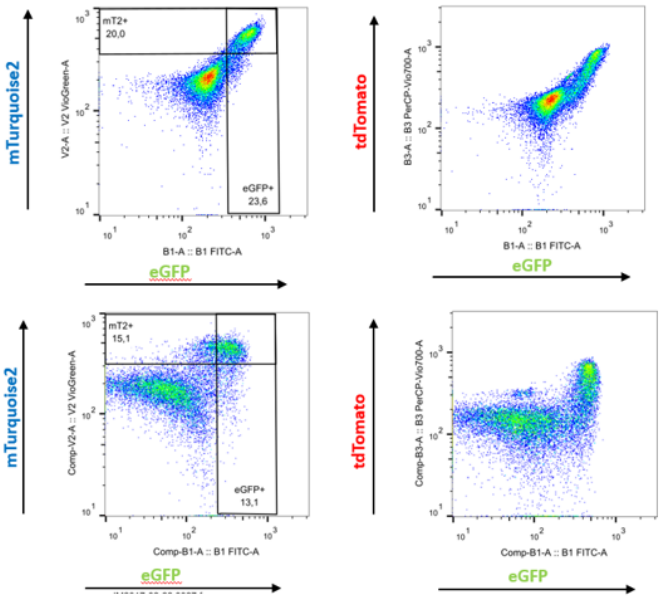

Figure 8. Effect of Fluorescence compensation on two-colour experiment: 200ng of mT2 and EGFP (left column) and 200ng of tdTomato and EGFP (right column) was transfected into A549 and fluorescence signal was determined in non-compensated (first row) and compensated (second row) channels.

Thus, bandpass filter and detector determine the channel of every measured fluorescent protein (Tung et al. 2004). Since fluorescent proteins have broad emission peaks, emission spectrum is not restricted to their allocated channel (Tung et al. 2004). Hence, emitted fluorescence of one fluorophore may partly be collected by a channel dedicated to another fluorophore resulting in spillover (Tung et al. 2004).

The method of mathematically correcting spectral overlap of two or more fluorescent proteins or fluorescent dyes is called fluorescence compensation (Baumgarth und Roederer 2000).The purpose is to subtract spectral overlap in order to evaluate fluorescence emission of each fluorophore in its appropriate channel (Tung et al. 2004) Compensation can be achieved through inter-laser compensation during measurement using electronic circuitry of the flow cytometer or by application of computed transformation on data obtained from flow cytometry (Tung et al. 2004).

Challenges of fluorescence compensation

In flow cytometry, two major sources of variability exist:

- photon counting (counting error): intrinsic to the process of measurement
- digital error : results through analogue-to-digital conversion (Hawley et al. 2004).

Problems may occur regarding display of flow cytometry data due to inaccurate conversion from linear to logarithmic signal by the flow cytometer (Baumgarth und Roederer 2000). As fluorescence compensation is a subtraction process, some events may be depicted as events with negative values after compensation (Hawley et al. 2004). As log function is undefined at ≤ 0 negative and zero channel values are set to 1 through logarithmic conversion of signals (Hawley et al. 2004). Two major consequences arise from this problem. Firstly, events are plotted on the x-axis and secondly, data appears undercompensated as variability is no longer symmetric (Hawley et al. 2004). An approach to properly visualize compensated data is the use of new data transformation with defined axes which are linear above and below zero and logarithmic at higher positive and negative values (Tung et al. 2004).

In this context, a compensation matrix was generated by Julia Maier and Islam Abd-El Rahman, which was applied on flow cytometry data obtained from our multi-colour experiments with 3P-TOP. For further information and gating strategy see 3.7.

1.3.3 Luciferase reporter proteins and dual-luciferase assay

Luciferase reporter proteins are widely used to study promoter activity, signal transduction or other cellular activities (Nakajima und Ohmiya 2010). Luciferases visualize activity of promoters through bioluminescence which is the emission of light from a living organism produced by an internal biochemical reaction (Daunert und Deo 2006). In this reaction, an enzyme (luciferase) converts a substrate (D-luciferin or coelenterazine) in the presence of oxygen into a product accompanied by emission of light in the visible range of the electromagnetic spectrum (Greer und Szalay 2002; Badr und Tannous 2011). Besides oxygen, some luciferases need co-factors for this reaction such as ATP and Mg^{2+} (Badr und Tannous 2011) (figure 9).

In nature, luciferases are found in organisms such as bacteria, fungi, insects and in marine organisms (Tannous et al. 2005). Once expressed in cells, luciferases either remain in the cytoplasm (e.g. Firefly luciferase) or they are excreted (Gaussia luciferase, Renilla luciferase). Two types of kinetics of bioluminescence reaction exist: flash-type kinetics and glow-type kinetics. Some luciferases such as Gaussia luciferase (GLuc) or Renilla luciferase (RLuc) create a signal immediately after addition of substrate which decreases within seconds (flash-kinetics) (Tannous et al. 2005). Other luciferases e.g. Firefly luciferase (FLuc) produce luminescence signal for a longer period of time (glow-kinetics) (Badr und Tannous 2011).

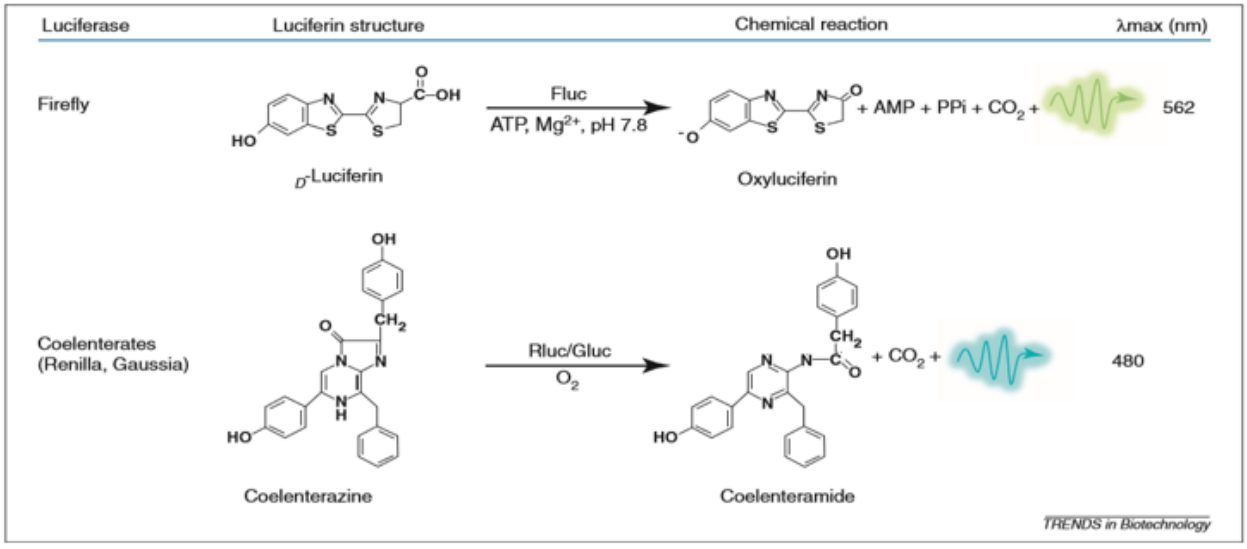

Figure 9. Bioluminescent reaction of FLuc, RLuc and GLuc: Luciferases (FLuc, RLuc, GLuc) convert their substrate (D-Luciferin, coelenterazine) into a product (oxyluciferin, coelenteramide) accompanied by the emission of light.
First row: Firefly luciferase (FLuc) oxidizes its substrate D-luciferin in the presence of oxygen, adenosine triphosphate (ATP), and Mg^{2+} into a non-reactive product called oxyluciferin whereby light is emitted with a peak of 562nm (Navizet et al. 2011; Tannous et al. 2005). Second row: Renilla luciferase (RLuc) and Gaussia luciferase (GLuc) catalyse the conversion of their substrate coelenterazine to coelenteramide which only requires molecular oxygen. Light is emitted with a peak of 480nm (Roda et al 2009; figure from Badr and Tannous 2011)

Firefly Luciferase (FLuc)

Originally isolated from American firefly, *Photinus pyralis*, Firefly luciferase (MW = 62 kDa) uses D-Luciferin as substrate and requires ATP and Mg^{2+} for this reaction (Tannous et al. 2005). FLuc is one of the most frequently used luciferases due to its high quantum yield, high sensitivity and broad linear range (Welsh und Kay 1997; Naylor 1999; Tannous et al. 2005)

Gaussia Luciferase (GLuc)

Gaussia luciferase from marine copepod *Gaussia princeps* (MW= 19.9 kDa) is the smallest of all luciferases and naturally secreted (Tannous et al. 2005). GLuc needs coelenterazine as substrate but no other co-factors except for molecular oxygen (Tannous et al. 2005). In addition, humanized GLuc has stronger signal intensity (200 fold) in cell culture compared to humanized forms of FLuc and RLuc (Tannous et al. 2005).

Dual luciferase assay

Luciferases with well-separated emission spectra are essential for performance of Dual reporter gene assay (Roda et al. 2009). In dual-reporter assays, an additional luciferase expressed under the control of a strong, constitutively active promoter (e.g. CMV or SV40) is used as internal control. The aim is to normalize light intensity of one luciferase with signal intensity of another luciferase with high expression level. In this way experimental variability due to variations in transfection efficiency or other effects is reduced (Nakajima und Ohmiya 2010).

In our experiments, Firefly Luciferase was used to measure promoter activity while Gaussia luciferase was used for normalization of Firefly luciferase results (see 3.11)

2 Aim of the thesis

The aim of this thesis was to assess function of our fluorescent reporter gene construct 3P-TOP which comprises three pathway-dependent promoters of Wnt, Notch and Hedgehog pathways fused to downstream fluorophores. Our reporter construct was transfected into lung cancer cell line A549 which was treated with pathway-specific activators to induce promoter activity. If pathways were activated, increased fluorescence signal would be measured via flow cytometry. In this way, activation of developmental signalling pathways can be dynamically visualized in cancer cells.

After assessing function of our reporter construct, we tested pathway-specificity of each promoter comparing their inducibility to the respective mutated versions of the promoter. For this purpose, we compared different cancer cell lines, pathway-specific activators, treatment modalities, timepoints for read-out and reporter gene assays. Hence, we established different workflows suiting each pathway-specific promoter.

Wnt, Notch and Hedgehog are highly conserved developmental signalling pathways often deregulated in different types of tumours. In future applications, our reporter construct could provide information about which of these pathways is deregulated and to which extent these pathways interfere with each other in tumour-derived cells. In addition, our reporter construct could also be used *in vivo* to non-invasively gain information about deregulated signalling pathways in different tumour types visualized by reporter genes as fluorescent proteins or luciferases.
In this way, impact of signalling pathways in oncogenesis can be better understood. Consequently, new approaches of cancer treatment can be developed to eradicate cancer more specifically in cancer patients and to reduce relapse rate.

3 Materials and methods

3.1 Materials and technical equipment

Following technical equipment was used for all methods described:

- Cell culture microplate, 96 well, PS, F-bottom, TC, white (Cat. No. 655098) and transparent (Cat. No. 655180) (Cellstar®, Greiner Bio-One)
- Cell culture flasks (83.3910.002/11.002/12.002. Sarstedt, Nümbrecht, Germany)
- Micropipettes (Eppendorf Research Plus)
- Multi-Channel Ultra High-Performance Pipettor, 12-Channel Pipettor, 50 to 300µl (Cat. No. 89134-758. VWR)
- F1-ClipTip™ Multichannel Pipette, 12-channel, 10 to 100µl (Cat. No. 4661170. Thermo Scientific) •
- Centrifuge Tube 15ml (Cat. No. E1415-0200. Starlab) and 50ml (Cat. No. E1450-0200. Starlab)
- Hemocytometer (Paul Marienfeld GmbH & Co. KG, Germany)
- Serological pipettes 5ml, 10ml, 25ml (Sarstedt)
- Water bath (Memmert GmbH + Co. KG)
- Inverted microscope (AE31 Elite Trinocular, Motic)
- Heracell™ 150i CO2 Incubator (Thermo Fisher Scientific)
- Heraeus Megafuge 16R Centrifuge (Thermo Fisher Scientific)
- Herasafe™ KS (NSF) Class II, Type A2 Biological Safety Cabinet (Thermo Fisher Scientific)
- Freezer -80°C (REVCO ExF, Thermo Scientific)
- MacsQuant® Analyzer 10 (Cat.No.130-096-343. Miltenyi Biotec)
- Plate reader (Infinite® M200 Pro, Tecan)
- Plate shaker (Eppendorf ThermoMixer®C, 05-412-503. Eppendorf)
- Ultrasonic cleaner (waterbath), (470105-414. VWR®, Radnor, PA, USA)
- Syringe filters, cellulose acetate, 0.22µm (Cat. No. 28145-477. VWR)
- pH meter (WTW)

Following materials were used in cell culture:

Name	Product number, supplier, location
Bovine Serum Albumin (BSA)	A9647. Sigma-Aldrich®, St. Louis, MO, USA
Dulbecco's Modified Eagle's Medium-high glucose	D5671. Sigma-Aldrich®, St. Louis, MO, USA
Dulbecco's Phosphate Buffered Saline (PBS)	D8537. Sigma-Aldrich®, St. Louis, MO, USA
Fetal Bovine Serum (FBS)	F7524. Sigma-Aldrich®, St. Louis, MO, USA Lot No. 064M3396
D (+)-Glucose	346351. Merck Milipore®, Darmstadt, GER
L-Glutamin, 200 mM	G7513. Sigma-Aldrich®, St. Louis, MO, USA
4-(2-hydroxyethyl)-1-piperazineethanesul-fonic acid (HEPES)	A3724.0500. VWR®, Radnor, PA, USA
Linear polyethylenimine (LPEI) 10 kDa	In house production by A. Taschauer et al.
MQ-Water, autoclaved	Arium® pro VF, Sartorius
Passive Lysis buffer, 5x	E194A, Promega®, Madison, WI, USA
Penicillin-Streptomycin (PenStrep)	P0781. Sigma- Aldrich®, St. Louis, MO, USA
RPMI-1640	R0883. Sigma- Aldrich®, St. Louis, MO, USA
Sodium hydroxide	A6829.1000. Applichem®, Darmstadt, DE
TrypLE™ Express (1x)	12605010. Gibco®, Grand Island, NY, USA

Table 1. Reagents used in cell culture

3.2 Plasmid DNA used in transfection experiments

Reporter plasmid	Pathway/ biological action	Mutated version	Assay	Product number, supplier
3P-TOP: pMuLE_EXPR_CMV-eGFP_TOP-iRFP_hPTCH1-mTurquoise2_CBF-tdtomato	Wnt, Notch, HH	no	FL	Cloned by Julia Maier in MMCT Lab, University of Vienna
Cbf:H2b-Venus	Notch	no	FL	Addgene plasmid #44211. Cambridge, MA, USA
pMULE_ENTR_CBF_tdTomato_L3-L2	Notch	no	FL	cloned by Julia Maier from original Addgene plasmid
cbfREMuteGFP	Notch	yes	FL	Addgene plasmid #26870. Cambridge, MA, USA
M50 Super 8x TOPFlash	Wnt	no	FLuc	Addgene plasmid # 12456. Cambridge, MA, USA
M51 Super 8x FOPFlash	Wnt	yes	FLuc	Addgene plasmid # 12457. Cambridge, MA, USA
pCTP4eGFPLuc	Wnt	no	FLuc	Gift from Kai Lipinsky , Keele University, UK
hPTCH-wt-Luc	HH	no	FLuc	Gift from Fritz Aberger, University of Salzburg
hPTCHMutLuc	HH	yes	FLuc	Gift from Fritz Aberger, University of Salzburg
pCMVGLuc	Constitutively active	/	GLuc	New England Biolabs®, Germany
peGFPLuc (CMV)	Constitutively active	/	FLuc	Clontech, Mountain View, USA
pUC19	/	/	/	Addgene plasmid #50005. Cambridge, MA, USA

Table 2. Plasmid DNA used in transfection experiments: abbreviations: FL=Fluorescence assay, FLuc=Firefly luciferase assay, GLuc=Gaussia luciferase assay

3.3 Pathway-dependent activators

Name	Class	Species	Pathway	Product number, supplier
EFhICN1 from original EFhICN1.CMV.eGFP*	pDNA	human	Notch	plasmid # 17623 from Linzhao Cheng, Addgene®
pCAGGS-NICD	pDNA	murine	Notch	plasmid # 26891 from Nicholas Gaiano, Addgene®
Wnt3A, recombinant	protein	human	Wnt	5036-WN, R&D Systems, Minneapolis, MN, USA
Sonic hedgehog (shh), recombinant	protein	human	Hedgehog	1845-SH, R&D Systems, Minneapolis, MN, USA

Table 3. Pathway activators of the Wnt, Notch and Hedgehog pathways:
*restriction digest was performed with EFhICN1.CMV.eGFP to cut out the CMV.eGFP cassette. Subsequently, the plasmid was ligated, transformed and verified. EFhICN1 was used as Notch activator in our experiments.

- Wnt3A: According to manufacturer, wnt3A was reconstituted to a concentration of 200µg/ml. For this purpose, 10µg of recombinant human wnt3A were dissolved in 50µl freshly prepared sterile PBS/0.1% bovine serum albumin. Five aliquots of 10µl were prepared and stored at -20°C.

- Shh: According to manufacturer, shh was reconstituted to a concentration of 100µg/ml. Hence, 25µg of recombinant human protein were dissolved in 250µl of freshly prepared sterile PBS/0.1% BSA. Five aliquots of 50µl were prepared and stored at -20°C.

3.4 Cancer cell lines and cell maintenance

Cancer cell lines

The human epithelial lung carcinoma cell line A549 (CRM-CCL-185TM, ATCC®, Manassas, VA, USA) was originally derived from a 58-year-old Caucasian male. A549 cell line was used for transfection experiments of our reporter plasmid 3P-TOP and also for testing of Notch-sensitive promoter CBF. This cell line was chosen due to its general suitability for various transfection experiments. Commonly, A549 were split in a ratio of 1:15 and the passage number was 118 for pathway activation in 3P-TOP. Cells were grown in fully formulated RPMI-1640 (+10% FBS, +1 % P/S, +2% L-glutamine).

The HeLa cell line (CCL-2™, ATCC®, VA, USA) is a human epitheloid cervix carcinoma cell line originally isolated from 31-year-old Henrietta Lacks in 1951 (https://en.wikipedia.org/wiki/HeLa). HeLa cells were used for assessing promoter activity of CBF (Notch) and TOPFlash (Wnt). Commonly, HeLa cells were split in a ratio of 1:6 and the passage numbers were 9-25; after thawing of new cells 9-14 respectively. Cells were cultivated in DMEM high glucose supplied with 10% FBS, 1% P/S and 2% L-glutamine.

NIH 3T3 cell line (CRL-1658™, ATCC®, VA, USA) is an embryonic fibroblast cell line derived from a Swiss mouse embryo. This cell line was used for promoter testing of hPTCH1-wt (Hedgehog). Cells were split regularly in a ratio of 1:8 and the passage numbers for our experiments were +1 to +16; after thawing of new cells, +3 to +8. Concerning the fact that this cell line was a gift, the passage number was not noted on cryogenic vial. For this reason, we started counting from +1 after thawing. NIH 3T3 cells were grown in fully formulated DMEM high glucose (10% FBS, 1% P/S and 2% L-glutamine).

Cell maintenance

A549, HeLa and NIH 3T3 cells were grown in 25/75/150 cm^3 cell culture flasks filled with fully formulated DMEM high glucose or RPMI-1640 depending on the cell line. The cells were cultivated at 37°C and 5% CO_2 in a humidified incubator. Upon 80-90% confluency, cells were split. For this purpose, cell culture medium was aspirated and cells were washed carefully with 1/2/3 ml PBS. Detachment of the cells was done with 0.5/1/1.5ml of TrypLe™. To achieve detachment, cells were incubated for 4min at 37°C and 5% CO_2. Through gentle tapping of the culture flask, cells were detached which was subsequently confirmed under microscope. In order to collect the cells, 2.5/5/7ml of appropriate cell culture medium was added and the cell suspension was transferred into a centrifuge tube. Hereafter, centrifugation was performed for 5min at 200 x *g* at room temperature. The supernatant was aspirated and the cell pellet resuspended in 1000µl of appropriate cell culture medium. Depending on splitting ratio, the desired fraction of cells was transferred into a new cell culture flask containing already the appropriate amount of cell culture medium prewarmed to 37°C, and incubated.

3.5 Transfection via LPEI based polyplexes

General transfection workflow of our experiments:

1. Day 1: Cell seeding into a 96-well plate (10.000 cells/well)
2. Day 2: Generation of LPEI based polyplexes and actual transfection of cells, treatment with pathway-specific activators
3. Day 3: Read-out via flow cytometry (FL=Fluorescence assay) or plate reader (BL=Bioluminescence assay)

The first day, 10.000 cells were seeded per well into a white (BL) or transparent (FL) 96-well plate. For this purpose, cells were processed as described in 3.4 until a pellet was generated. The cell pellet was resuspended in 1000µl of appropriate cell culture medium. From this cell suspension, a 1:10 dilution was made with PBS and cells were counted with hemocytometer (Neubauer chamber). Subsequently, each well was seeded with the appropriate amount of cell suspension and filled up with cell culture medium to a volume of 200µl. In general, four or five wells per condition were prepared and cells were incubated at 37°C and 5% CO_2 for 24h.

The following day, solutions for generation of polyplexes were prepared in 500µl Eppendorf tubes. Solution I contained our transfection reagent linear polyethylenimine (LPEI in HBG, 10kDa, c= 1575ng/µl and LPEI in HBS, 10kDa, c=1843 ng/µl) diluted in either HBG (20mM HEPES/5 % (w/V) sodium, pH 7.4) or HBS (20 mM HEPES/5 % (w/V) glucose, pH 7.4). Solution II contained 400ng or 800ng of plasmid DNA (pDNA) diluted in the same buffer as LPEI. Polyplexes were always generated at N/P ratio of 9 in all of our experiments. Here an example of calculations for generation of polyplexes:

For transfection of 4 wells, 50µl of polyplex solution were prepared which means that 10µl were prepared extra to compensate possible pipetting errors. This volume (50µl) consists of equal amounts of solution I (25µl) and solution II (25µl). For example, 200ng of pDNA (c= 232.5µg/ml) and LPEI (c= 1575ng/µl→ 1:5 dilution was prepared with MQ-water resulting in c= 315µg/ml) were used to form polyplexes at N/P ratio of 9 resulting in 3.72µl LPEI diluted in 21.28µl HBS (solution I) and 4.30µl pDNA diluted in 20.70µl HBS (solution II). In this way, solution I and solution II were prepared for each condition.

Before polyplexes were generated, cells were taken out from the incubator and cell culture medium was aspirated. Instead, 90µl of basal medium (DMEM high glucose or RPMI-1640 without any supplements) was added per well. Polyplexes were generated through flash pipetting technique in the following way:
The micropipette was adjusted to 3/4 of total volume comprised of solution I and II (50µl in total). Hence, it was adjusted to 37.5µl. Solution I (LPEI in buffer) was pipetted up resulting in a pipette tip filled with air. The air was carefully released until the solution reached the end of the tip which was dipped into solution II (pDNA in buffer). The solutions were rapidly pipetted up and down for 20 times (flash pipetting) which guaranteed mixing of the solutions. As a general rule, LPEI solution was added to the pDNA solution and not vice versa.

From 50µl of polyplexing solution, 10µl were added per well. Each well already contained 90µl of basal medium resulting in 100µl in total. The 96-well plate was incubated for 4h at 37°C and 5% CO2. After incubation, cells were provided with fully supplemented cell culture medium and treated with pathway specific activators:

- Activation of 3P-TOP: cells were treated with 100µl cell culture medium or 100µl cell culture medium containing 1) wnt3A, 2) co(wnt3A), 3) shh, 4) co (shh)
- Activation of Notch: 100µl of fully supplemented medium was added (pathway activators were co-transfected)
- Activation of Wnt: cells were treated with 100µl of cell culture medium or 100µl cell culture medium containing 1) wnt3a, 2) co (wnt3A), 3) LiCl
- Activation of Hedgehog: 100µl of cell culture medium was added or 100µl cell culture medium containing 1) shh, 2) co (shh)

Wnt3A was used in different concentrations:

- Activation of 3P-TOP: c= 1.2 ng/µl
- Wnt experiments: c= 200 ng/µl

Shh was used in different concentrations:

- Activation of 3P-TOP: c= 0.5 ng/µl
- Hedgehog experiments: c= 1 ng/µl

After treatment, cells were incubated at 37°C and 5% CO_2 for 24h. Read-out was performed on day 3 via flow cytometry (see 3.6) or plate reader (see 3.10).

3.6 Flow cytometry and gating strategy without compensation

Read-out via flow cytometry

Read-out was performed 24h after transfection via flow cytometry (MACS QUANT® Analyzer 10, MACS Milteny Biotec). FACS was switched on at least 30min before actual measurement. Meanwhile, cells were detached in the following way:

Cell culture medium was aspirated and cells were washed with 200µl PBS/well. For detachment of the cells, 20µl TrypLE™ was added per well and cells were incubated for 4min at 37°C and 5% CO_2. 180µl PBS was added per well and cells of each well were resuspended 2-3 times with a pipette to ensure detachment and homogenisation of cell suspension.

After detachment of cells, the 96-well plate was brought to FACS and placed onto a cooling rack, which was kept previously at +4°. The lid of the 96-well plate was removed.
Thereupon, adequate settings were chosen on the FACS device:

Rack/F-bottom 96-well plate: MACSPLEX Filter Plate
Flow rate: high
Mode: fast

Uptake volume was set to 150µl whereas sample volume was set to 200µl in order to prevent formation of air bubbles in the process of sample uptake. In addition, cell suspension of each well was mixed manually with a pipette to ensure that cells were well distributed and not laying on the bottom of the wells. Channels were chosen accordingly.

Data obtained from flow cytometry was analysed with FlowJo X (version 10.0.7, www.flowjo.com, Ashland, Oregon, USA) and both *.fcs and *.mqd files were saved. For analysis of our experiments, the *.mqd data files were used. The results were visualized via Graphpad Prism (version 6.02, www.graphpad.com, La Jolla, CA, USA) and statistical significance was determined with two-tailed, unpaired t-test.

Gating strategy using non-compensated channels:

Data from experiments evaluated without compensation matrix was gated the following way:

The first gate (SSC-A/FSC-A) gates out cell debris. In that way, only whole cells are used for further analysis. From these cells, doublets are gated out (FSC-A/FSC-H) resulting in single cells. From single cells, fluorescent signals are gated in channels assigned to each fluorescent protein (table 5)

An example of gating strategy using non-compensated channels is depicted in figure 10. This gating strategy was used in our Notch activation experiments as these were performed using only one fluorescent protein per condition. In addition, 3P-TOP experiments were also evaluated with non-compensated channels in order to compare the results with compensated data.

Excitation laser	Channel	Emission filter*	Fluorescent protein/parameter
Blue, 488nm	FSC	488/10 nm	size
	SSC	488/10 nm	granularity
Blue, 488nm	V1	450/50 nm	mTurquoise2
	V2	525/50 nm	
Blue, 488nm	B1	525/50 nm	EGFP, Venus
	B2	585/40 nm	
Blue, 488nm	B2	585/40 nm	tdTomato
	B3	655-730 nm	
Red, 635 nm	R1	655-730 nm	iRFP
	R2	750 nm LP*	

Table 5. Overview of MACSQuant instrumental configuration used for our fluorescent proteins:
* emission filters measure a certain range of wavelengths, e.g. B1 channel (525/ 50 nm) measures light emission in the range of 500-575 nm
** LP is the abbreviation of long pass filter which allows transmission of light from 750 nm and higher wavelengths
(Information of instrumental configurations provided by MiltenyBiotech)

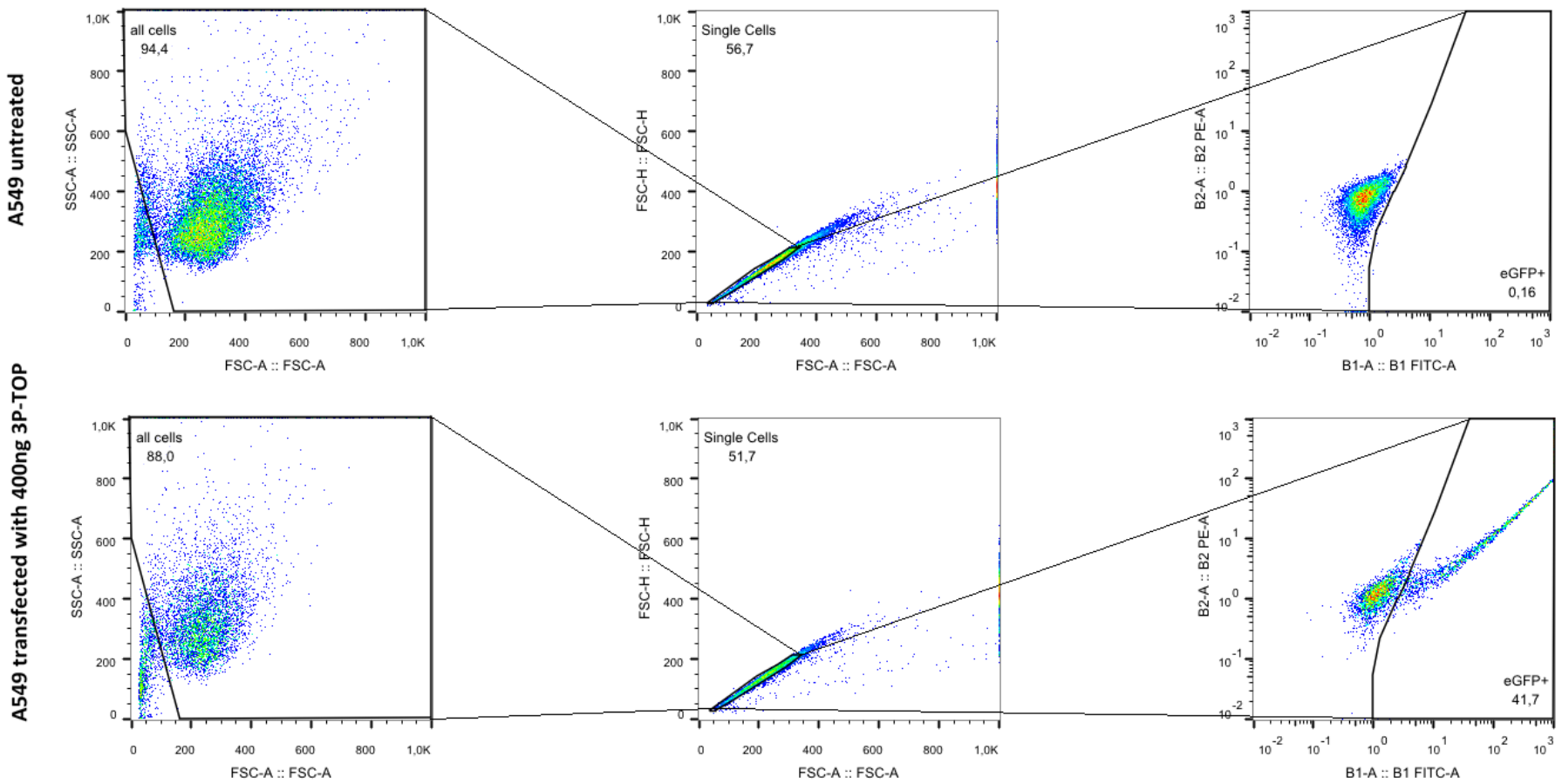

Figure 10. Gating strategy of Untreated (first row) and 400ng 3P-TOP transfected (second row) A549 cells without compensation: first column: the first gate "all cells" excludes cell debris at the left bottom; second column: gate "single cells" eliminates doublets. Hence, only single cells are used to determine fluorescence signal in appropriate channels; third row: eGFP positive cells are gated out with B1-A/B2-A channels providing information about transfection efficiency of our reporter construct, 3P-TOP. Untreated cells (first row) were 0,16% eGFP positive which is at autofluorescence level. In contrast, A549 cells transfected with 400ng 3P-TOP were 41,7% eGFP positive.

3.7 Compensation matrix and gating strategy with compensation

In order to evaluate our reporter construct 3P-TOP, which comprises four fluorescent proteins, a compensation matrix was applied on flow cytometry data before software analysis with FlowJo X (www.flowjo.com, Ashland, Oregon, USA).

For creation of compensation matrix, following experiment was conducted by Julia Maier and Islam Abd El Rahman (Abd El Rahman 2017):
Four reporter plasmids containing a fluorophore gene (EGFP, mTurquoise2. tdTomato, iRFP) downstream of CMV promoter were transfected into A549 cells. The constitutive active CMV promoter was used to guarantee equal expression level of all fluorescent proteins used. Cells were transfected with each fluorophore alone, double-transfections and finally multi-transfection of three or four fluorophores. Untreated cells not expressing any fluorescent protein were used to determine level of autofluorescence. Light emission of each fluorophore was measured in its respective filter, then in the filters assigned to other fluorophores. Spectral interferences among the fluorophores were observed and evaluated statistically. Hereinafter, a compensation matrix was generated by Julia Maier and Islam Abd El Rahman for evaluation of our multi-colour experiment with 3P-TOP.

The flow cytometer (MACS QUANT® 18 Analyzer 10. MACS Milteny Biotec) used in all of our fluorescence assays is equipped with violet (405nm), blue (488nm) and red (635nm) excitation lasers. It comprises a 10-channel system of two scatter (FSC, SSC) and 8 fluorescent channels.
Table 6 provides an overview of spectral characteristic of our fluorescent proteins, their assigned channels and channels which were compensated for spectral overlap among them.

Fluorescent protein	Excitation	Emission	Channels	Compensated channels
mTurquoise2	434 nm	473 nm	V2-A/ V1-A	comp. V2-A/ comp. B1-A
EGFP	488 nm	507 nm	B1-A/ B2-A	comp. B1-A/ comp. V2-A
tdTomato	554 nm	581 nm	B3-A/ B2-A	comp. B3-A/ comp. R2-A
iRFP	690 nm	713 nm	R2-A/ R1-A	comp. R2-A/ comp. B3-A

Table 6. Spectral characteristics of fluorescent proteins and their assigned channels

Gating strategy with compensation

Evaluation with compensated channels leads to a cell population which looks different than the cell population looks in non-compensated channels. For this reason, a different gating strategy was used for compensated data:

The first two gates remained the same: The first gate (SSC-A/ FSC-A) excludes cell debris while the second gate eliminates doublets from single cells. Out of single cells, fluorescence signal of all fluorescent proteins is gated with quadrant gate which is divided into four subset gates. Percentage of cells from two horizontal subset gates in upper part of the plot correspond to the channel on y-axis. In contrast, percentage of cells from two vertical subset gates in right part of the plot correspond to channel on x-axis. The percentage of both subset gates was summed up as both represent fluorescence emission of a fluorescent protein in the respective compensated channel. Quadrant gates were used instead of polygon gates as this method was more suitable for detection of fluorescence positive events. An example of gating strategy with compensation matrix is shown in figure 11.

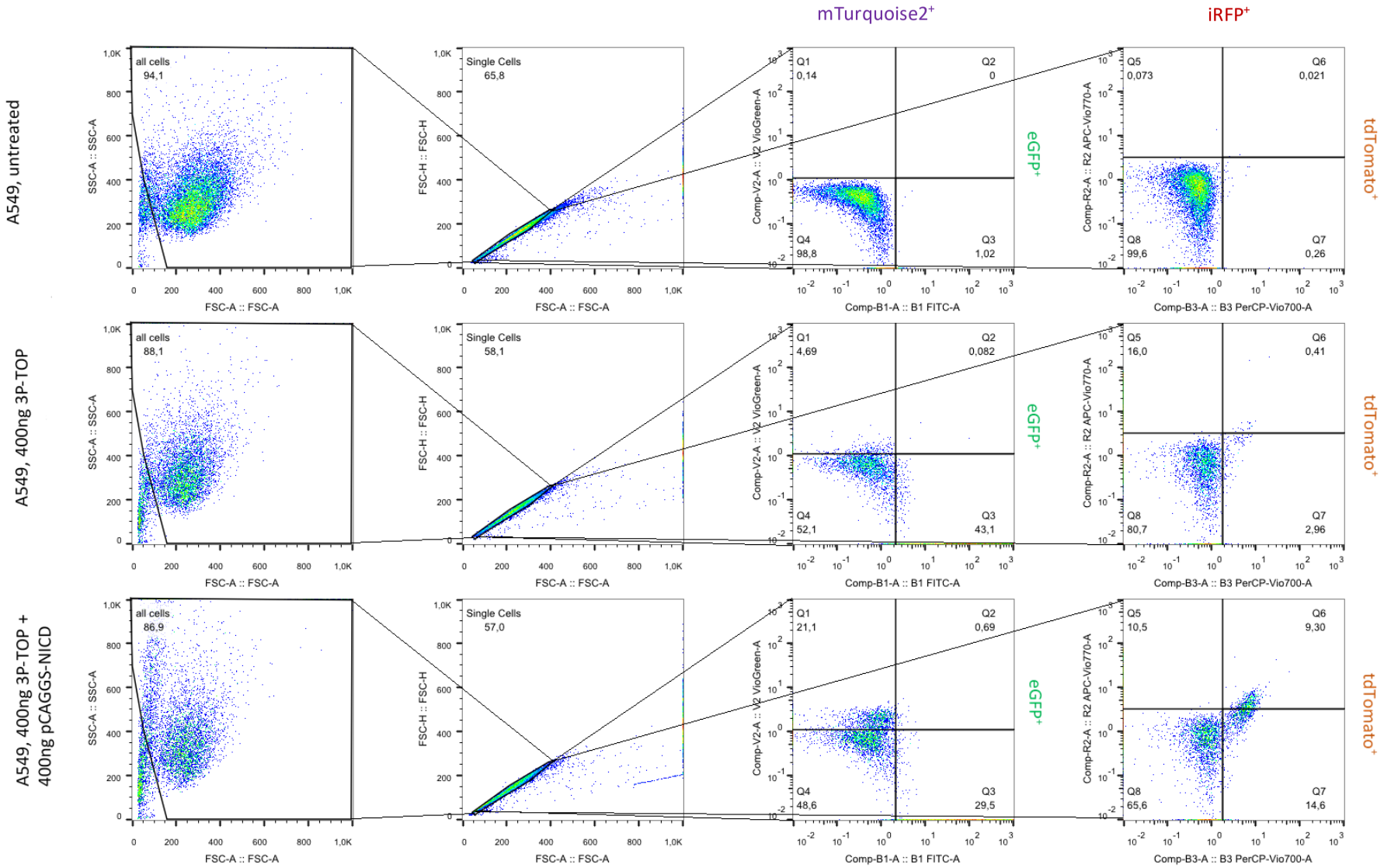

Figure 11. Gating strategy with compensation of untreated (first row), 400ng 3P-TOP transfected (second row) and 400ng 3P-TOP + 400ng Notch activator transfected A549 cells: first column: "all cells" gate excludes cell debries; second column: "single cells" gate eliminates doublets; third column: quadrant gate: Q2 and Q3 represent eGFP+ cells in comp. B1-A while Q1 and Q2 represent mT2+ cells in comp. V2-A; fourth row: quadrant gate: Q6 and Q7 represent tdTomato+ cells in comp. B3-A while Q5 and Q6 represent iRFP+ cells in comp. R2-A

3.8 In-house preparation of luciferin assay buffer (hLAB) for Firefly luciferase assay

Firefly luciferase requires certain co-factors such as ATP or Mg^{2+} besides D-luciferin for production of luminescence. In bioluminescent assay, luciferase is provided with its substrate and co-factors from a buffer. For our experiments, housemade luciferase assay buffer (hLAB) was used.

Two possible approaches exist regarding usage of this buffer:

- In-house prepared buffer is prepared separately and frozen at -80°C. Before Firefly luciferase assay is performed, housemade buffer is thawed and D-luciferin added resulting in hLAB or
- The complete housemade luciferase assay buffer (hLAB) is prepared in advance and frozen at -80°C. Before luminescence measurement, hLAB is thawed and used as such.

For time saving reasons, frozen complete hLAB was used in our experiments. Two hours before luminescence measurement via plate reader, hLAB was kept in a dark place at room temperature to thaw. If buffer was left over after an experiment, it was frozen again and reused a second time with no relevant loss in activity which was previously confirmed in our laboratory.

For our experiments, hLAB was used prepared by Katharina Müller according to the protocol established in the MMCT lab (Müller et al. 2019).

<u>Preparation of housemade luciferin assay buffer (adapted from Müller 2017):</u>

Reagents:

- Glycylglycine (Cat. No. G-3915. Sigma-Aldrich)
- Magnesium chloride 6xH2O (Cat. No. A4425. AppliChem)
- Ethylenediaminetetraacetic acid (Cat. No. E-6758. Sigma-Aldrich)
- Coenzyme A (trilithium salt) (Cat. No. C3019. Sigma-Aldrich)
- L-Dithiothreitol (Cat. No. D9779. Sigma-Aldrich)
- ATP (Cat. No. 10519979001. Roche Diagnostics GmbH, Austria)
- Luciferin powder (Na-salt, Promega)
- Sodium hydroxide (Cat. No. 55881. Sigma-Aldrich)
- Hydrochloric acid (HCl) (Cat. No. 13778-150. Sigma-Aldrich)
- MQ-water (Arium®pro VF, Sartorius)

The following stock solutions were prepared according to the protocol of Müller et al. 2019.
All of them except for glycylglycine stock solution can be prepared in advance and stored at recommended storage temperatures:

- Stock solution 1: 20ml of 1 M Glycylglycine pH 8.0
- Stock solution 2: 50ml of 100mM $MgCl_2$
- Stock solution 3: 50ml of 500mM EDTA pH 8.0
- Stock solution 4: 2.5ml Coenzyme A (42.6 mg/ml)

- Stock solution 5: 48ml of 10mM luciferin (prepared under light protection)

In a Schott Duran® bottle, 10ml of freshly prepared Glycylglycine stock solution (1M) and 5ml of $MgCl_2$ stock solution (100nM) were mixed together. 100µl of EDTA stock solution (500mM) was added. 254mg DTT and 139mg ATP were weighed separately in Eppendorf tubes, each was dissolved in 1ml MQ-water and added to the mixture. To ensure that everything was transferred, Eppendorf tubes were washed with 4ml MQ-water which was again transferred to the mixture. 2.5ml Coenzyme A was added and 472ml MQ-water poured in the Schott Duran® bottle. pH was adjusted to 8.2 and MQ-water was added to the final volume of 500ml. The solution was filtered through a 0.22µm cellulose acetate filter.
Finally, 25ml of D-luciferin stock solution (10mM) was added to the 500ml prepared giving the solution a greenish-yellow colour. Centrifuge tubes (15ml) were wrapped up with aluminum foil to protect the buffer from light. 5ml and 10ml aliquots were prepared and frozen at -80°C

3.9 In-house preparation of coelenterazine assay buffer (hCAB) for Gaussia Luciferase assay

Gaussia luciferase from marine copepod *Gaussia princeps* requires coelenterazine as substrate. Hence, coelenterazine buffer is needed for bioluminescence measurement via plate reader. In addition, buffer provides Gaussia luciferase with sodium chloride needed for this biochemical reaction due to its marine occurrence.

In our experiments, in-house produced coelenterazine assay buffer (hCAB) was prepared according to the protocol of Tannous et al. (Tannous 2009) and stored at -80°C. Before read-out via plate reader, hCAB was thawed in a waterbath for 30min at room temperature. Since hCAB is prone to auto-oxidation, it should not be left thawed for a longer period of time.

<u>Preparation of in-house produced coelenterazine assay buffer (adapted from Müller 2017):</u>

Reagents:

- Coelenterazine (Cat. No. s053. Synchem UG & Co., Germany) stock solution (5 mg/ml; in acidified methanol)
- Dulbecco's Phosphate Buffered Saline (Cat. No. D8537. Sigma-Aldrich)
- Sodium chloride (Cat. No. A2942.5000. Applichem)
- Sodium hydroxide (Cat. No. A6829.1000. Applichem), NaOH dilution

For preparation of PBS/5mM NaCL (pH 7.2): 29.22mg sodium chloride was dissolved in 90ml PBS. pH was adjusted to 7.2. PBS was added to total volume of 100ml. The solution was filtered through a 0.22µm cellulose acetate filter.

Following steps were carried out under light protection: Centrifuge tubes (15ml) were wrapped up in aluminum foil. Aliquots of 3ml, 6ml and 8ml were prepared:

For an aliquot of 6ml, 20.33µl coelenterazine stock solution (5mg/ml) was added to 5.98ml of PBS/5mM NaCl resulting in 20µM of in-house produced coelenterazine assay buffer (hCAB). Aliquots were frozen at -80°C. Residuals were frozen and reused a second time.

3.10 Dual luciferase assay with Firefly luciferase and Gaussia luciferase

Firefly luciferase was chosen to visualize promoter activity of TOPFlash (Wnt) and hPTCH1-wt (Hedgehog) For normalization of measured FLuc activity, a second reporter plasmid containing Gaussia luciferase driven by CMV promoter was co-transfected. Read-out of FLuc and GLuc assays was performed 24h after transfection via plate reader (Infinite® M200 Pro, Tecan). Expressed FLuc remains intracellularly whereas GLuc is secreted into cell culture medium. For this reason, FLuc assay requires a cell lysis step in contrast to GLuc assay. Both assays were performed on the same day.

Prior to luminescence measurement, cells were seeded in a white 96-well plate and transfected as described in 3.5. 24h after transfection, cells were processed as described below before measurement.

Following facts were considered in advance:

- hLAB was thawed for 2h in dark place at room temperature
- hCAB was thawed for 30min at room temperature in a water bath
- Plate reader was switched on at least 30min before measurement
- Passive lysis buffer, 5x, (PLB), previously stored at -20°C, was thawed for 20min at room temperature and diluted to 1x PLB with MQ-water

Firstly, cells were processed for measurement of GLuc activity, afterwards for measurement of FLuc activity:

24h after transfection, cells (plate I) were taken out from the incubator. The supernatant (cell culture medium) was carefully resuspended 2-3 times with a micropipette adjusted to 30µl. This step is required to swirl up Gaussia luciferase from the bottom of the well. 20µl of supernatant were transferred into a new white 96-well-plate (plate II). Plate II was used for measurement of GLuc activity. Meanwhile, the original white 96-well-plate (plate I) was incubated at 37°C and 5% CO_2. Measurement at the plate reader is described below.

Finishing measurement, plate I was processed in the following way for measurement of Fluc activity: The remaining supernatant was transferred into a transparent 96-well-plate (plate III), wrapped up with parafilm and frozen at -80°C in case a second measurement of GLuc activity was needed. Cells were washed with 200µl PBS/well and 30µl of 1x Passive Lysis buffer was added per well to lyse the cells. Subsequently, the 96-well-plate was fixed with adhesive tape onto plate shaker (Eppendorf ThermoMixer®C, 05-412-503. Eppendorf). The 96-well plate was shaken at 500 RPM for 30min at room temperature. Cell lysis was confirmed by visual control under microscope (shrunken cell aggregates should be visible). After lysis, luminescence measurement followed at the plate reader.

Read-out via plate reader

I-control™-Microplate Reader Software was opened and the respective measurement protocol (either FLuc assay or GLuc assay) selected. The system was washed 1x Aqua purificata, 1x 70% EtOH and 1x Aqua purifcata. Thereafter, it was primed 2x with air and substrate needle was dried carefully with tissue. Finally, it was primed 2x with substrate (either hCAB or hLAB). The 96-well plate was inserted into the plate reader without the lid. Wells to be measured were marked on the template.

Following settings were used at each measurement:
Injection volume: 50µl for GLuc and 100µl for FLuc
Speed: 200µl/sec
Refill speed: 100µl/sec
Wait time: 2 sec
Integration time: 10.000 msec

After luminescence measurement, data was saved and the system washed with 1x Aqua purificata, 1x 70% EtOH and primed 2x 70% EtOH. Substrate needle was left in 70% EtOH for 5min. Finally, the system was washed 2x Aqua purificata.

3.11 Evaluation of Dual luciferase assay

Bioluminescence signal measured by plate reader is depicted as relative light unit (RLU). For evaluation of promoter inducibility, FLuc activity was normalized with GLuc activity. Normalized results were expressed as the ratio of Firefly to Gaussia luciferase activity.

$$\textit{Normalized RLU} = \frac{RLU(FLuc)}{RLU\ (GLuc)}\ x\ 10.000$$

The results (normalized RLU) were visualized via Graphpad (Prism version 6.02. www.graphpad.com, La Jolla, CA, USA) and depicted as means ± SD (n=4). Statistical significance was determined with two-tailed, unpaired t-test.

4 Results

4.1 Reporter construct 3P-TOP was partly inducible with pathway activators via fluorescence assay

For activation of Notch, Wnt, Hedgehog pathways in our reporter construct 3P-TOP, A549 cells were seeded (day 1) and transfected (day 2) with different amounts of 3P-TOP (200ng, 400ng or 800ng/well) to compare transfection efficiency.

For activation of Notch in 3P-TOP, cells were co-transfected with Notch-sensitive activator:

- 200ng 3P-TOP and 200ng pCAGGS-NICD (2ng/µl)
- 400ng 3P-TOP and 400ng pCAGGS-NICD (4ng/µl)

Read out for transfection efficiency and Notch pathway activity was done 24h after transfection via flow cytometry (day 3).

For activation of Wnt and Hedgehog, cells were transfected with 400ng 3P-TOP (day 2) and treated with their respective pathway activator 24h after transfection (day 3):

- wnt3A (c=1.2ng/µl) or co(wnt3A) of the same concentration
- shh, (c=0.5ng/µl) or co(shh) of the same concentration

Both loading controls [co(wnt3A and co(shh)] contained PBS +0.1% BSA of the same concentration as activators and cell culture medium. PBS +0.1% BSA is the reconstitution solution for wnt3A and shh protein (see 3.3).

Read-out of Wnt and Hedgehog activity was performed 24 hours after activator treatment via flow cytometry (day 4).

Data was evaluated with FlowJo X (www.flowjo.com, Ashland, Oregon, USA) with compensation matrix (4.1.1) and without compensation (4.1.2).

4.1.1 Evaluation of 3P-TOP with compensation

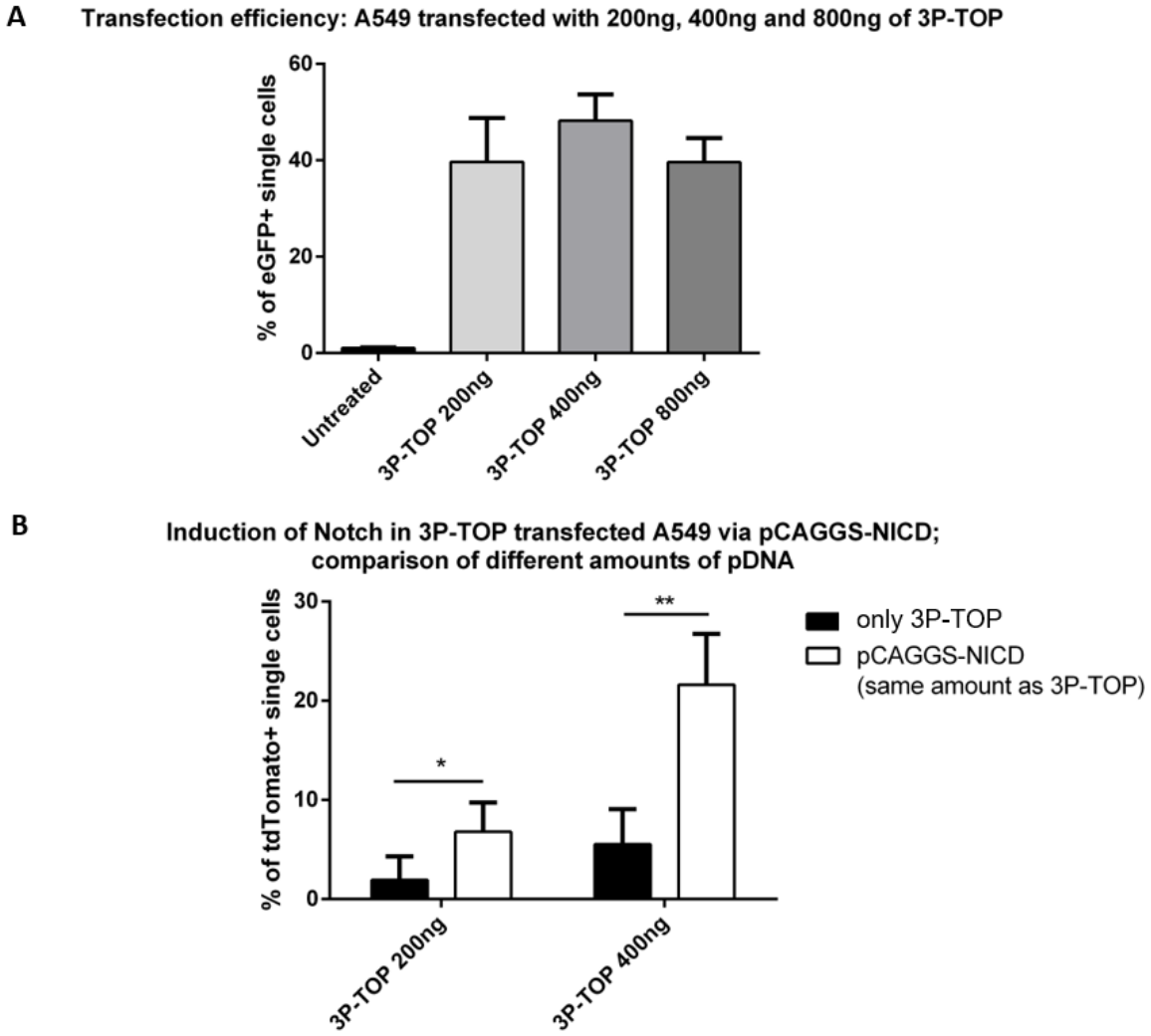

Figure 12. Determination of transfection efficiency and activation of Notch pathway via pCAGGS-NICD in 3P-TOP transfected A549: A) Highest transfection efficiency was obtained with 400ng 3P-TOP (48.2%) compared to 200ng (39.6%) and 800ng (39.6%). Transfection efficiency is determined by percentage of eGFP$^+$ cells. B) Either 200ng 3P-TOP and 200ng pCAGGS-NICD or 400ng 3P-TOP and 400ng pCAGGS-NICD were co-transfected. Higher increase in Notch activity was observed with 400ng pCAGGS-NICD (21.6%) than with 200ng pCAGGS-NICD (6.8%). Notch activation is determined by percentage of tdTomato$^+$ cells.

<u>Highest transfection efficiency with 400ng 3P-TOP (figure 12)</u>

Different amounts of 3P-TOP (200ng, 400ng, 800ng) were transfected to determine the best transfection efficiency defined by percentage of eGFP$^+$ cells (comp. B1-A/ comp. V2-A). Cells transfected with 400ng 3P-TOP had the highest percentage of eGFP$^+$ cells (48.2%) compared to cells which were transfected with 200ng (39.6%) or 800ng (39.6%).

More significant increase in Notch pathway activity with 400ng of murine Notch activator, pCAGGS-NICD (figure 12)

In order to activate Notch pathway, cells were co-transfected with murine Notch activator, pCAGGS-NICD: either 200ng 3P-TOP and 200ng pCAGGS-NICD (2ng/µl) or 400ng 3P-TOP and 400ng pCAGGS-NICD (4ng/µl) were used per well for transfection. Increase in Notch activity is defined by increase in percentage of tdTomato$^+$ cells (comp. B3-A/ comp. R2-A).
Our results revealed a higher increase of Notch pathway activity in cells co-transfected with 400ng of Notch activator (21.6%) compared to cells which were co-transfected with 200ng of Notch activator (6.8%).
Aside from that, transfection of 400ng 3P-TOP without activator resulted in higher percentage of tdTomato$^+$ cells (5.53%) than cells transfected with 200ng 3P-TOP (1.93%).

No induction of Wnt or Hedgehog pathway with respective activators (figure 13)

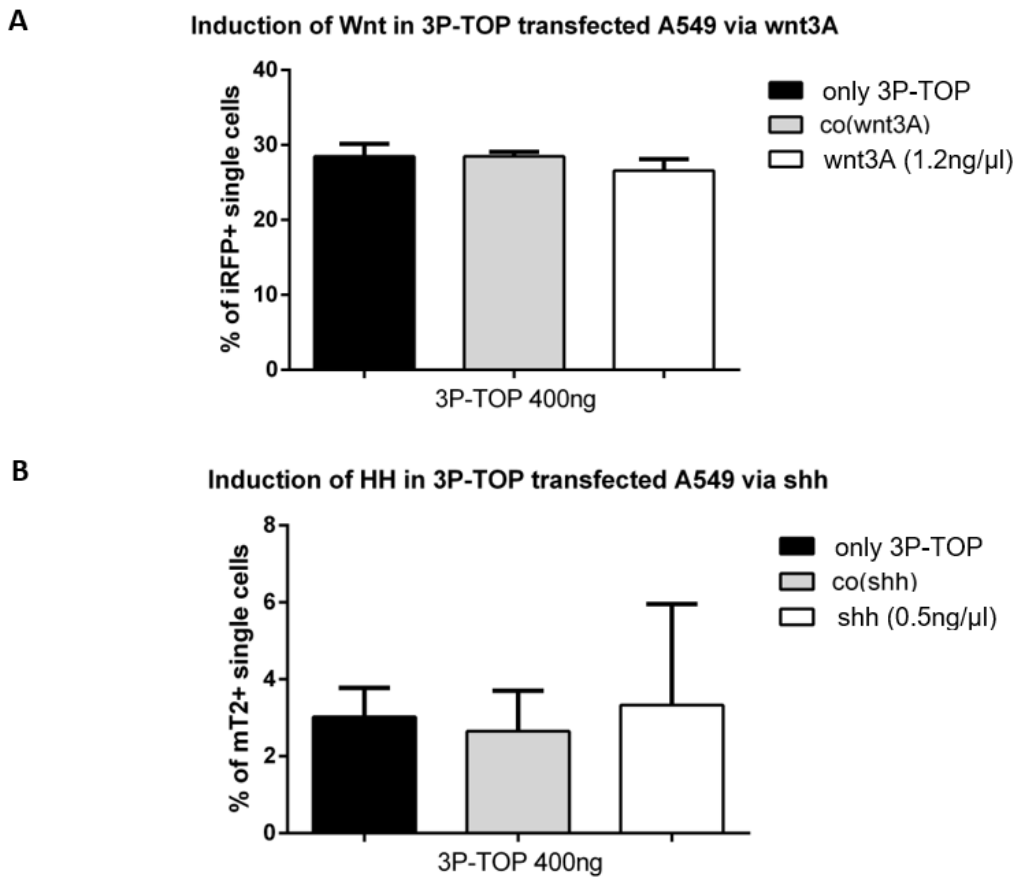

Figure 13. Activation of Wnt and Hedgehog pathways in 3P-TOP transfected A549 cells with respective pathway activator: A) For activation of Wnt pathway, cells were treated with wnt3A (1.2ng/µl) and compared to loading control co (wnt3A). Wnt activation is determined by an increase of iRFP$^+$ cells. No increase in signal was measured upon treatment with activator. B) For activation of Hedgehog pathway, cells were treated with shh (0.5ng/µl) and compared to loading control co(shh). Hedgehog activation is determined by an increase of mTurquoise2$^+$ cells. No increase in signal was detectable upon treatment with pathway activator.

For activation of the Wnt pathway, cells were treated with recombinant wnt3A protein (1.2ng/µl) or loading control co(wnt3A). Increase in Wnt activity is determined by an increase in $iRFP^+$ cells (comp. R2-A/ comp. B3-A). No increase in signal was detected in cells treated with wnt3A. Surprisingly, cells which were transfected only with reporter construct and received no further treatment were 28.5% iRFP positive. The high number of $iRFP^+$ cells may result due to gating strategy (quadrant plot) as iRFP signal was usually very low in our experiments.

For activation of Hedgehog pathway, cells were treated with recombinant shh protein (0.5ng/µl) or loading control co(shh). Increase in Hedehog activity was determined by an increase in $mTurquoise2^+$ cells. No increase in signal was measured in cells which were treated with shh (3.5%) compared to cells which received loading control (2.65%).

To summarize, transfection efficiency of 3P-TOP was highest with 400ng of transfected reporter construct, and Notch-dependent promotor (CBF) was inducible with the murine Notch activator pCAGGS-NICD. Wnt and Hedgehog- dependent promoters (TOPflash and hPTCH1) of our reporter construct were not inducible upon activation treatment with recombinant protein. For this reason, promoter function of TOPFlash and hPTCH1 was assessed with luciferases instead of fluorescent proteins in the following experiments. Promoter function of CBF (Notch) was further tested with fluorescence assay.

4.1.2 Evaluation of 3P-TOP without compensation

Comparable transfection efficiency and Notch activation without compensation (figure 14)

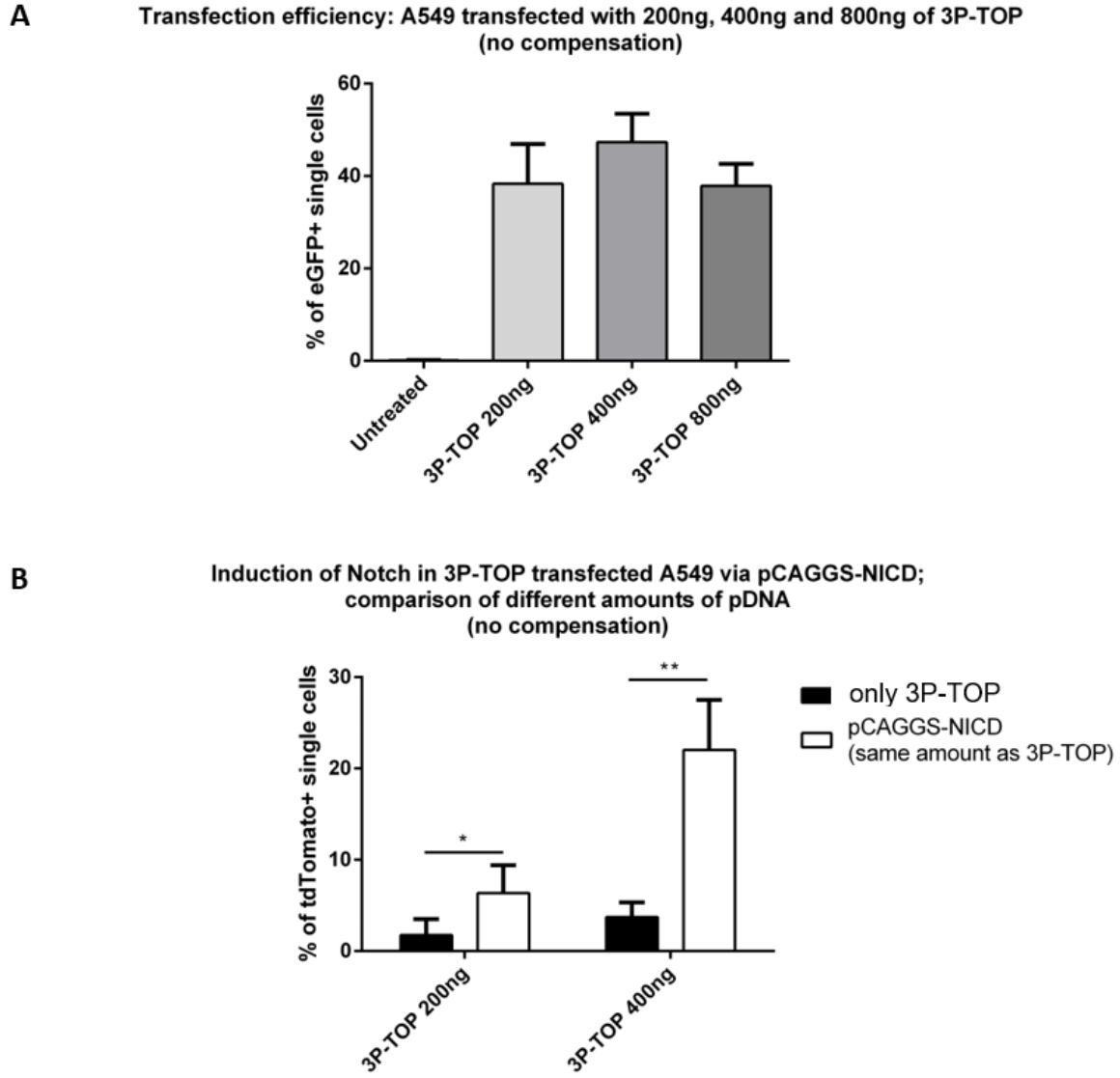

Figure 14. Determination of transfection efficiency and Notch activation via pCAGGS-NICD in 3P-TOP transfected A549 without compensation: A) Highest transfection efficiency was obtained with 400ng 3P-TOP (47.3%) compared to 200ng (38.3%) and 800ng (37.9%). Transfection efficiency was determined as percentage of eGFP$^+$cells (B1-A/B2-A) B) Either 200ng 3P-TOP and 200ng pCAGGS-NICD or 400ng 3P-TOP and 400ng pCAGGS-NICD were co-transfected. Higher increase of Notch activity was obtained with 400ng pCAGGS-NICD (22.1%) than with 200ng pCAGGS-NICD (6.4%). Notch activation was determined by percentage of tdTomato$^+$cells (B3-A/ B2-A).

Comparable transfection efficiency and Notch activation without compensation (figure 14)

Although gating strategy (3.6.) was different for evaluation of 3P-TOP without compensation, results of transfection efficiency and Notch activation with murine Notch activator pCAGGS-NICD were comparable:

Transfection efficiency, determined by percentage of eGFP$^+$ cells in B1-A/ B2-A channels, was highest in cells transfected with 400ng 3P-TOP (47.3%). With compensation, we received 48.2% eGFP$^+$ cells which is comparable. Notch activation was determined by an increase in percentage of tdTomato$^+$ cells (B3-A/ B2-A). We received again higher Notch activation in cells transfected with 400ng pCAGGS-NICD (22.0%) compared to cells transfected with 200ng of activator (6.4%).

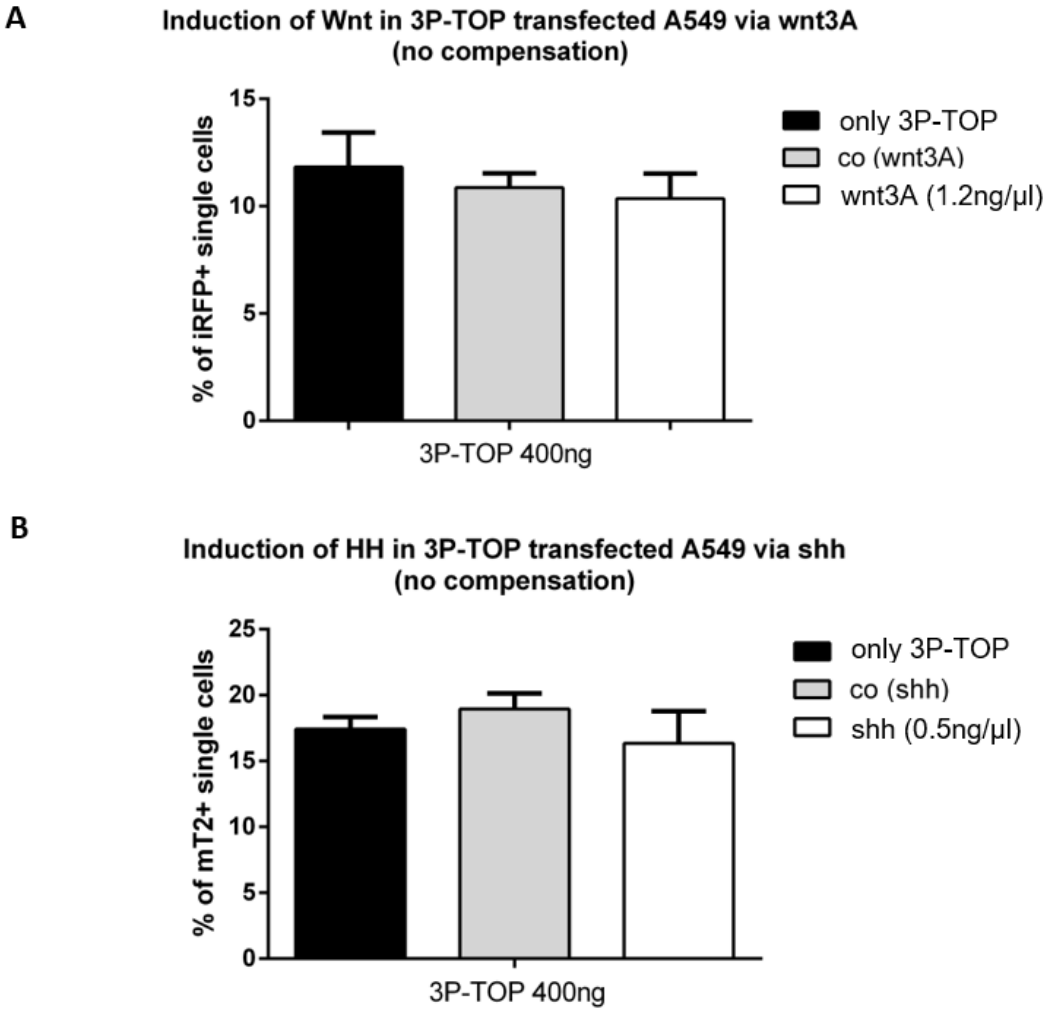

Figure 15. Activation of Wnt and Hedgehog pathways in 3P-TOP transfected A549 with respective activators without compensation: A) For activation of Wnt pathway, cells were treated with wnt3A (1.2ng/µl) and compared to loading control co(wnt3A). Wnt activation is determined by an increase of iRFP$^+$ cells (R2-A/ R1-A). . No increase in signal was measured upon treatment with activator. B) For activation of Hedgehog pathway, cells were treated with shh (0.5ng/µl) and compared to loading control co(shh). Hedgehog activation is determined by an increase in mTurquoise2$^+$cells (V2-A/ V1-A). No increase in signal was detectable upon treatment with activator.

Different percentages of fluorescent positive cells regarding Wnt and Hedgehog pathways (figure 15)

Either with compensation or without, no induction of Wnt and Hedgehog pathways in 3P-TOP was detectable. Interestingly, we received different percentages of fluorescent positive cells compared to the cells which were evaluated using compensation matrix:

Wnt activation:

- 10-12% iRFP$^+$ cells without compensation matrix (R2-A/ R1-A) compared to
- 26-29% iRFP$^+$ cells with compensated channels (comp. R2-A/comp B3-A);

Hedgehog activation:

- 16-18% mTurquoise2$^+$ cells without compensation matrix (V2-A/ V1-A) compared to
- 2-3% mTurquoise2$^+$ cells with compensated channels (comp. V2-A/ comp. B1-A)

Concerning Wnt pathway, we can only assume why we received more iRFP$^+$ cells with compensation. Earlier experiments revealed that iRFP expression in A549 cells is very low, especially if transfected in combination with other fluorescent proteins (Abd El Rahman 2017). As iRFP has its excitation (690nm) and emission (713nm) maxima in near-infrared range, it has the least influence of eGFP emission compared to tdTomato and mTurquoise2. Most probably, percentage of iRFP$^+$ cells is higher with compensation due to different gating strategy (quadrant plot instead of polygonal plot).
In regard to Hedgehog pathway, percentage of mTurquoise2$^+$ cell is lower if compensation matrix is used. As eGFP has a broad emission spectrum, it emits also light in V2-A channel which is assigned to mTurquoise2 (see 5.3).

4.2 Notch pathway

As CBF promoter was inducible in 3P-TOP, we continued testing of CBF promoter with fluorescent reporter by flow cytometry. We assessed promoter function by comparing pathway activation of CBF (cbf-H2B-Venus, cbf-tdTomato; 400ng each) with the mutated version (cbfREMuteGFP, 400ng) upon co-transfection with murine Notch activator (pCAGGS-NICD, 400ng) and human Notch activator (EFhICN1. 400ng). PUC19 was transfected as an additional negative control in order to see if co-transfection in general leads to signal increase. Cbf-H2B-Venus and cbfREMuteGFP were compared directly as Venus and eGFP have emission spectra in the same range. We compared two different cell lines (A549. HeLa) and we wanted to see if pathway activation also depends on the expressed fluorescent protein (Venus vs. tdTomato). For evaluation of fluorescence signal, no compensation was used as every condition contained only one expressed fluorescent protein: cbf-tdTomato was evaluated in B2-A/B3-A channels whereas Venus and eGFP were evaluated in B1-A/B3-A channels.

4.2.1 HeLa is a more suitable cell line for Notch pathway activation than A549

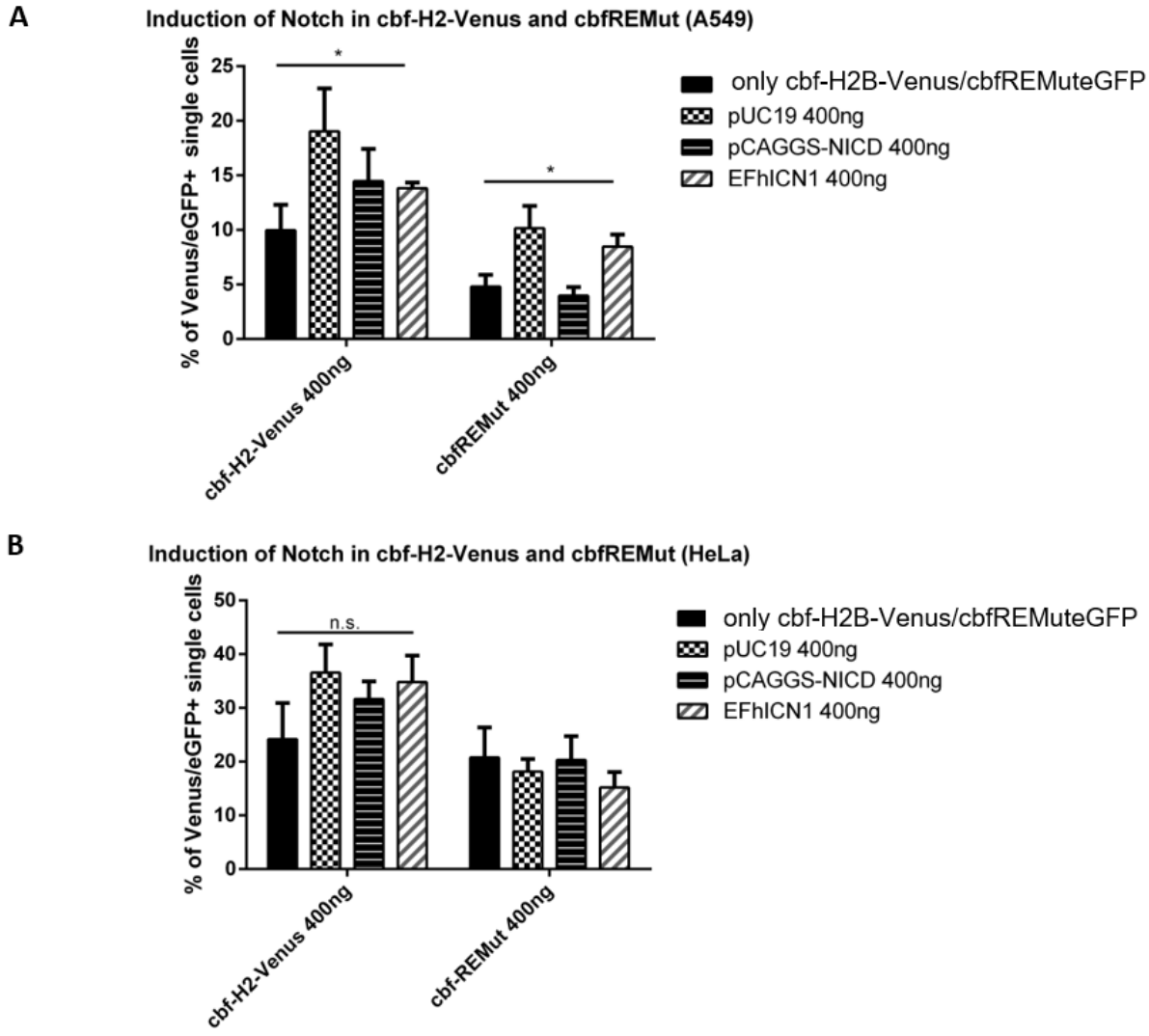

Figure 16. Notch activation in cbf-H2B-Venus and cbfREMuteGFP in two different cell lines: A) transfection in A549 B) transfection in HeLa
Cbf-H2B-Venus and cbfREMuteGFP (400ng each) were transfected in two different cell lines. Pathway activation was assessed due to co-transfection of Notch-dependent activators (pCAGGS-NICD and EFhICN1, 400ng each) and compared to negative controls (only cbf-H2B-Venus/cbfREMuteGFP; 400ng pUC19).

Comparison of inducibility of Cbf-H2B-Venus and cbfREMuteGFP in A549 and HeLa (figure 16)

Regarding cbf-H2B-Venus and the mutated version cbfREMut, we received in general a higher fluorescence signal in HeLa cells than in A549 cells: Transfection of 400ng cbf-H2B-Venus resulted in 24.2% Venus$^+$ HeLa cells and 10.0% Venus$^+$ A549 cells. CbfREMut is the negative version of CBF promoter which should not cause a higher signal due to Notch activators. In our experiment with HeLa cell line, all conditions containing cbfREMuteGFP have a similar percentage of eGFP$^+$ cells (15-20%). By contrast, A549 cells transfected with cbfREMUTeGFP and EFhICN1 were 8.5% eGFP$^+$ compared to cells which received any Notch activator (4.8% eGFP$^+$).

Higher percentage of tdTomato$^+$ cells in HeLa than in A549 (figure 17)

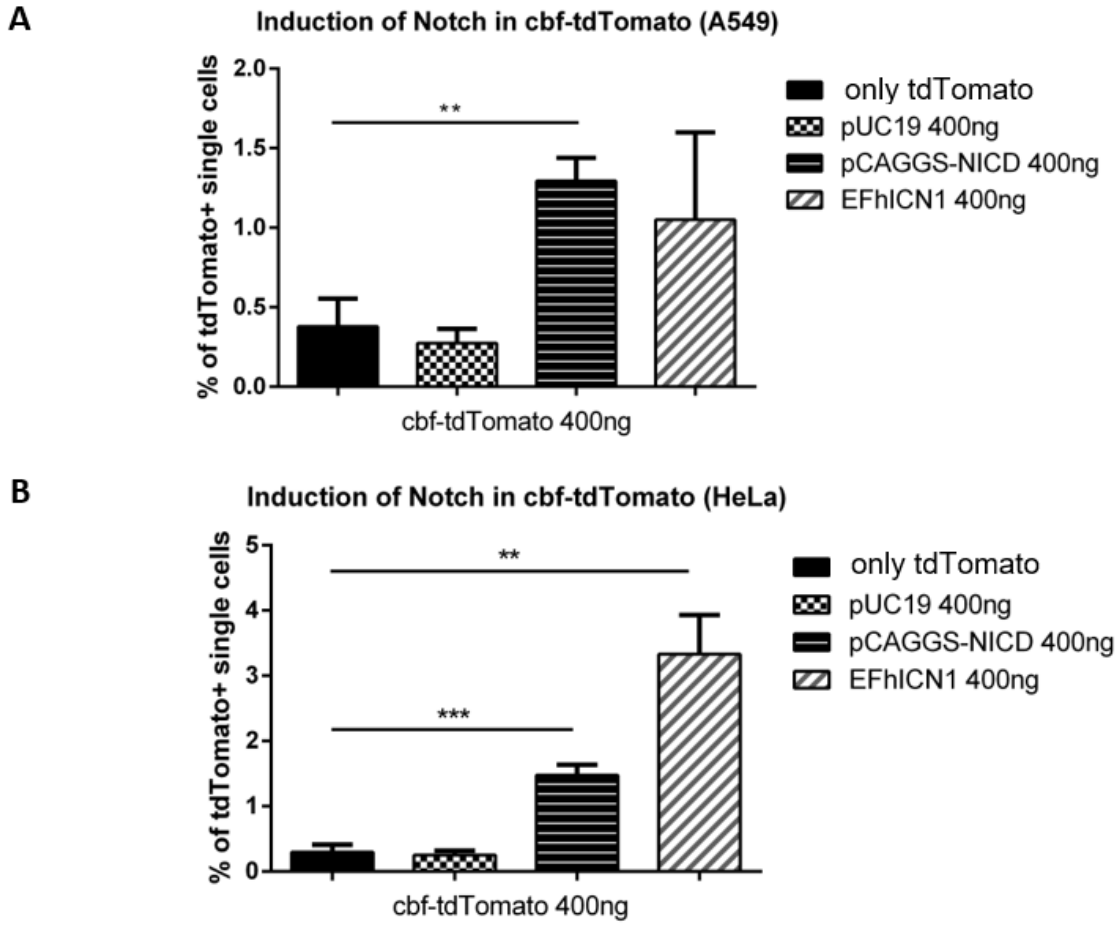

Figure 17. Notch Activation in cbf-tdTomato in two different cell lines: A) transfection in A549 B) transfection in HeLa**.** 400ng cbf-tdTomato was transfected in two different cell lines. Pathway activation was assessed due to co-transfection of Notch- dependent activators (pCAGGS-NICD and EFhICN1, 400ng each) and compared to negative controls (only cbf-tdTomato, 400ng pUC19).

Transfection of 400ng cbf-tdTomato resulted in 0.38% tdTomato$^+$ A549 cells whereas co-transfection of 400ng cbf-tdTomato and 400ng murine Notch activator pCAGGS-NICD resulted in 1.3% tdTomato$^+$ A549 cells. By contrast, 0.3% of HeLa cells were tdTomato$^+$ which were transfected with 400ng cbf-tdTomato and co-transfection of 400ng cbf-tdTomato and 400ng human Notch activator EFhICN1 resulted in 3.3% tdTomato$^+$ HeLa cells. To sum up, signal increase due to co-transfection with Notch activator was higher in HeLa cells than in A549 cells. For this reason, HeLa cell line was used for later Notch experiments.

4.2.2 Higher inducibility of CBF with tdTomato reporter instead of Venus

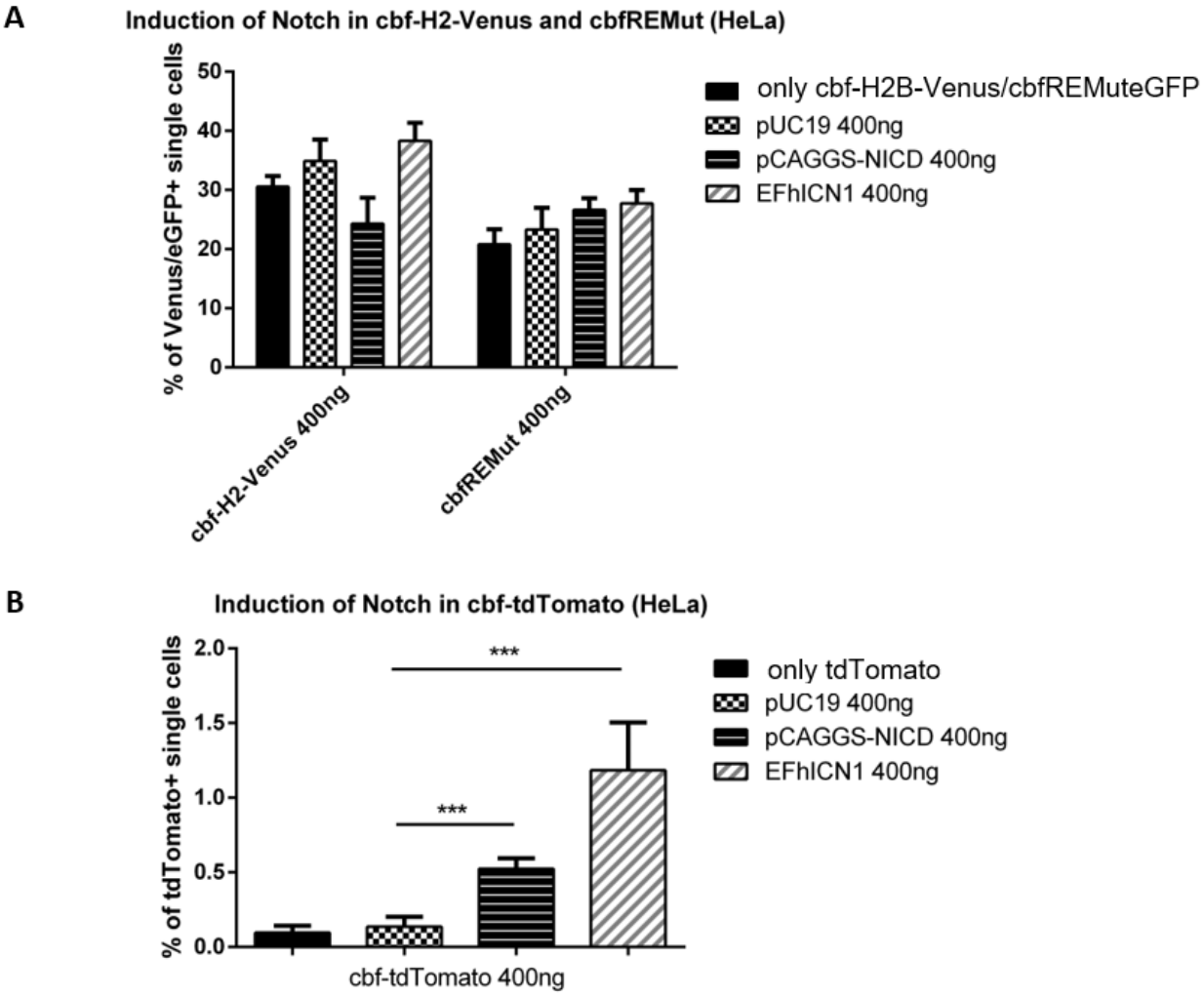

Figure 18. Notch activation in cbf-H2B-Venus, cbfREMuteGFP and cbf-tdTomato in HeLa cell line: A) Cbf-H2B-Venus and cbfREMuteGFP, 400ng each, were transfected into HeLa B) 400ng cbf-tdTomato was transfected into HeLa. Pathway activation was assessed due to co-transfection of Notch- dependent activators (pCAGGS-NICD and EFhICN1, 400ng each) and compared to negative controls (only cbf-H2B-Venus/cbfREMUTeGFP/cbf-tdTomato, 400ng pUC19)

Although fused to the same promoter (CBF) and expressed in the same cell line, our results revealed a significant difference in inducibility of CBF in dependence on which fluorescent reporter proteins was expressed (figure 18). HeLa cells transfected with 400ng cbf-H2B-Venus had a higher baseline signal (30.5% tdTomato$^+$) than HeLa cells transfected with 400ng cbf-tdTomato (0.1% tdTomato$^+$). Co-transfection with human Notch activator EFhICN1 resulted in 38.3% tdTomato$^+$ cells in condition "cbf-H2B-Venus" and 1.2% tdTomato$^+$ cells in condition "cbf-tdTomato". In case of cbf-tdTomato, signal increase is >1000% with human Notch activator EFhICN1 which is highly significant in contrast to cbf-H2B-Venus. Reporter construct cbf-tdTomato showed in our experiments higher Notch-sensitivity than cbf-H2B-Venus.

4.3 Wnt pathway

In order to assess function of our Wnt-dependent promoter, 200ng TOPFlash-Luc and 200ng of the mutated version FOPFlash-Luc were transfected into HeLa cells performing dual luciferase assay with FLuc and GLuc. Hence, every condition was a co-transfection with 200ng pCMVGLuc. For activation of Wnt pathway, cells were treated with wnt3A protein (200ng/µl) and compared to cells treated with loading control co(wnt3A) of the same concentration as wnt3A (1µg/ml). PUC19 was transfected as an additional negative control while CMVeGFPLuc was used as transfection control (positive control).
Inducibility of TOPFlash was compared to the inducibility of a second Wnt-dependent promoter, CTP4eGFPLuc. In addition, LiCl was tested as Wnt-dependent activator and compared to wnt3A. Read out was performed 24h after transfection via plate reader.

4.3.1 Comparison of two Wnt-dependent promotors: TOPFlash was more inducible than CTP4

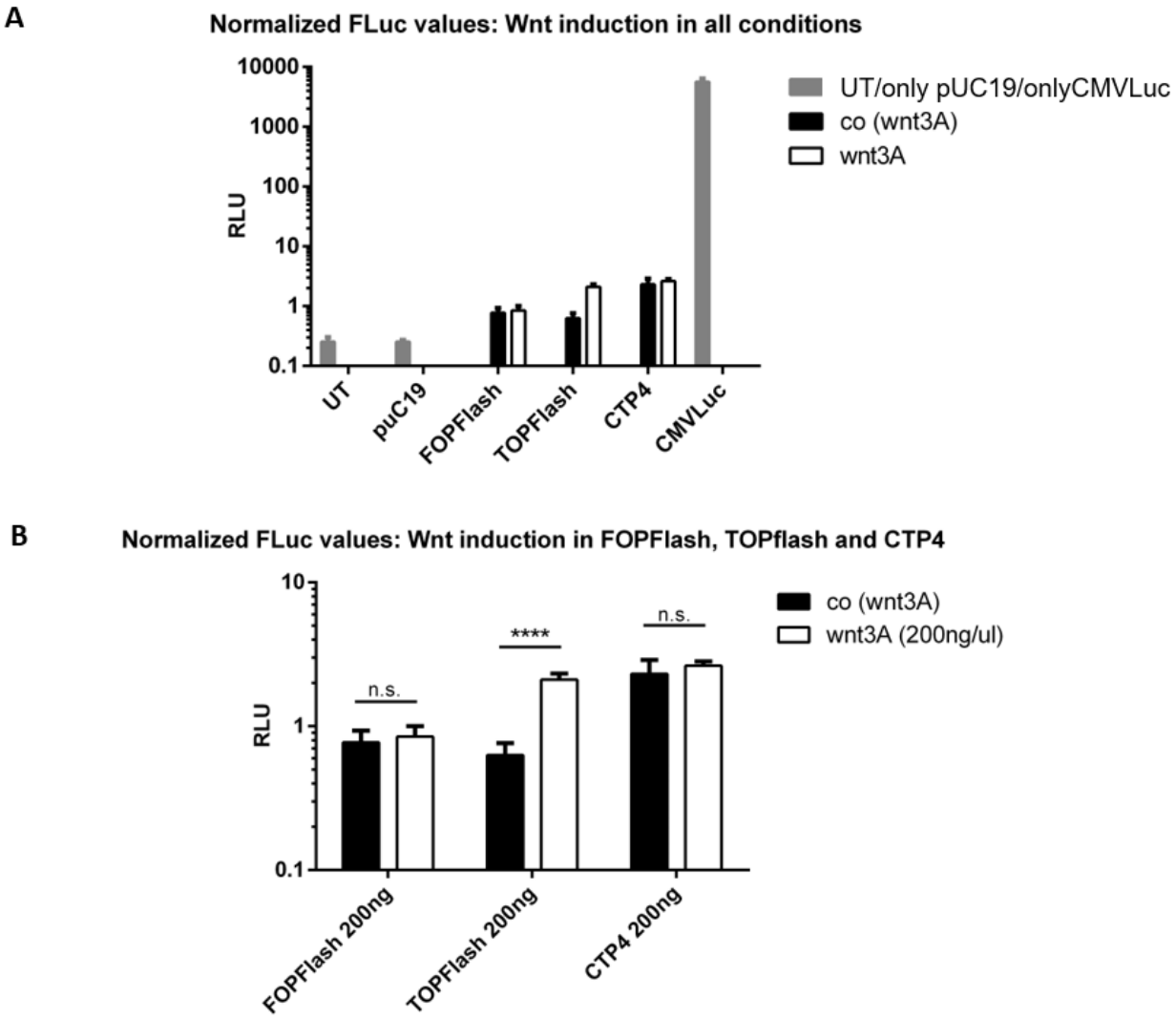

Figure 19. Wnt activation in TOPFlash, FOPFlash and CTP4 in HeLa: A) Normalized FLuc values of all conditions (UT= untreated cells, pUC19, FOPFlash, TOPFlash, CTP4, CMVLuc; 200ng each). B) Normalized Fluc values of two Wnt-dependent promoters (TOPFlash, CTP4) and FOPFlash, the mutated version of TOPFlash. 200ng of each promoter were transfected into HeLa cells. Pathway activation was assessed due to treatment with Wnt activator wnt3A (200ng/µl) 4 hours after transfection. Wnt activation was compared between cells which received wnt3A to cells which received loading control co(wnt3A).

Wnt-dependent promoter TOPFlash was highly inducible upon treatment with Wnt activator wnt3A (200ng/µl): Light intensity increased from 0.63 RLU in cells treated with loading control co(wnt3A) to 2.11 RLU in cells treated with wnt3A which is a highly significant increase in luminescence. Cells transfected with FOPFlash, the mutated version of TOPFlash, showed no relevant increase in signal upon wnt3A treatment.

By contrast, the second Wnt-dependent promoter CTP4 produced a higher baseline signal (3.0-3.7 RLU) than TOPFlash (0.6-2.1 RLU). Still, no significant increase in light intensity and thus pathway activity could be measured in cells trasnfected with CTP4 upon addition of wnt3A. Hence, TOPFlash promoter was more inducible than CTP4 promoter upon addition of Wnt protein wnt3A.

4.3.2 Wnt3A showed more Wnt pathway specificity than LiCl

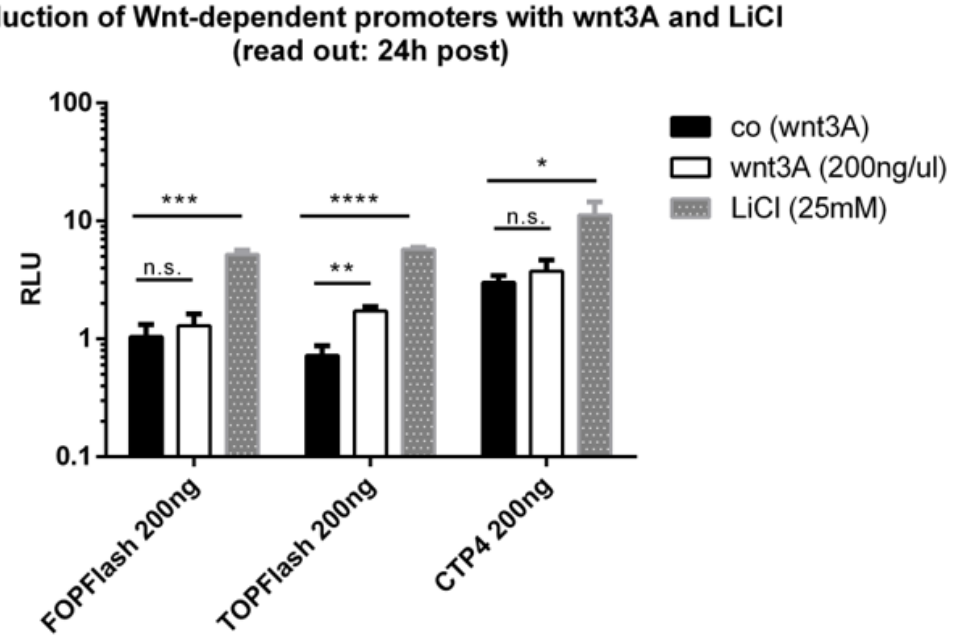

Figure 20. Wnt activation in TOPFlash, FOPFlash and CTP4 with two different Wnt activators (wnt3A and LiCl): Normalized FLuc values of TOPFlash, FOPFlash and CTP4. 200ng of each plasmid was transfecetd into HeLa cells. Pathway activation was assessed with two different Wnt activators, namely wnt3A (200ng/µl) and LiCl (25mM) and compared to loading control co(wnt3A).

LiCl, also used for activation of Wnt pathway, was compared to wnt3A for its Wnt-specificity. Light intensity of cells treated with 25mM LiCl and wnt3A (200ng/µl) was compared to cells which received loading control co(wnt3A). According to our results, wnt3A treatment increases light signal significantly only in TOPFlash (from 0.72 RLU to 1.72 RLU) but not relevantly in FOPFlash and CTP4. By contrast, LiCl treatment leads to an increase of signal in all promoters: FOPFlash (1.04 RLU to 5.21 RLU), TOPFlash (0.72 RLU to 5.76 RLU) and CTP4 (3.01 RLU to 11.25 RLU). Hence, LiCl led to an increase in bioluminescence in two Wnt-dependent promoters (TOPFlash, CTP4) but also in the mutated version FOPFlash which should normally have lower transcriptional activity than the original promoter. According to our results, wnt3A is a more specific Wnt activator than LiCl.

4.4 Hedgehog pathway

In order to assess function of our Hedgehog-dependent promoter, 400ng hPTCH1-wt-Luc and 400ng of the mutated version hPTCHMut-Luc were transfected into NIH 3T3 cells performing dual luciferase assay with FLuc and GLuc. Every condition was a co-transfection with 400ng pCMVGLuc. For activation of Hedgehog pathway, cells were treated with shh protein (1µg/ml) and compared to cells treated with loading control co(shh) of the same concentration as shh (1µg/ml). PUC19 was transfected as an additional negative control while CMVeGFPLuc was used as transfection control (positive control). Read out was performed 24h after transfection via plate reader

Two different treatment modalities (table 7) were used for our Hedgehog activation experiments with the purpose to use less of expensive Hedgehog activator shh protein:
The first three experiments (KP14, KP15, KP18) were performed as following: 4 hours after transfection supernatant was aspirated from each well and 50µl shh or 50µl loading control co(shh) were added (treatment 1). The other two experiments (KP19, KP20) were conducted as always: 4 hours after transfection, 100µl shh or 100µl loading control co(shh) were added per well (treatment 2).
Additionally, different amounts of pDNA were transfected: 800ng pDNA/well was used in KP14-15 and 400ng pDNA/well was used in KP18-20. The amount of pDNA was changed with the aim to reduce cell toxicity and thus to increase inducibility of hPTCH1-wt.

Hedgehog experiments	pDNA (ng) of promoter	total pDNA/well	50ul/well (treatment 1)	200ul/well (treatment 2)
KP14	400ng	800ng	yes	
KP15	400ng	800ng	yes	
KP18	200ng	400ng	yes	
KP19	200ng	400ng		yes
KP20	200ng	400ng		yes

Table 7. Different amounts of pDNA and different treatment modalities of our Hedgehog experiments

4.4.1 hPTCH1-wt was not significantly inducible with shh

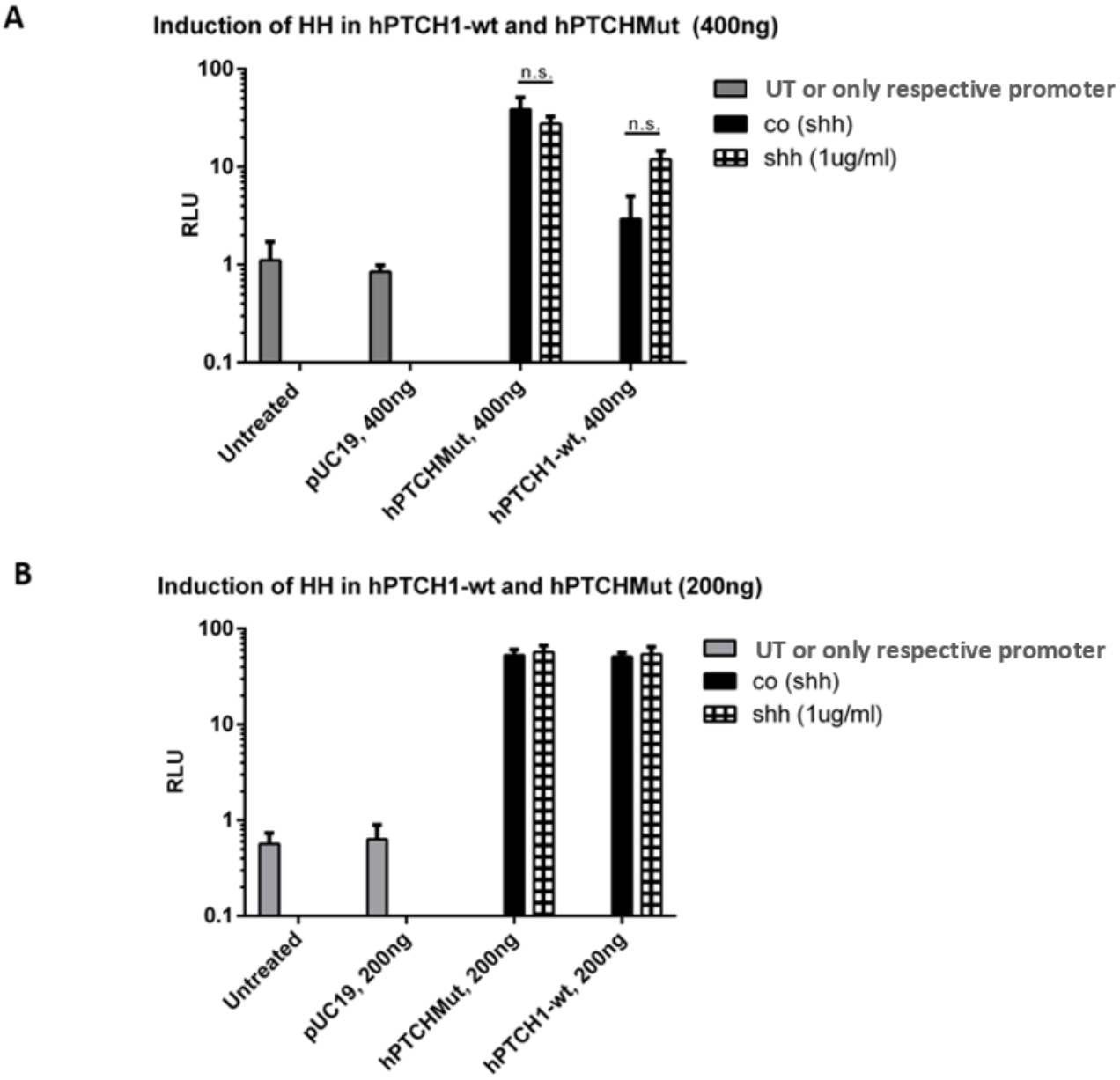

Figure 21. Activation of Hedgehog in hPTCH1-wt and hPTCHMut in NIH 3T3 cell line: A) Normalized FLuc values of all conditions (untreated cells, pUC19, hPTCHMut, hPTCH-wt). 400ng of each were transfected and cells were treated according to treatment 1 B) Normalized values of all conditions (untreated cells, pUC19, hPTCHMut, hPTCH-wt). 200ng of each were transfected and cells were treated according to treatment 2. Pathway activation was assessed with Hedgehog activator shh (1µg/ml) and compared to cells which received loading control co(shh).

Our results regarding inducibility of hPTCH1-wt with Hedgehog activator shh were not reproducible. Figure 21 shows the results of two Hedgehog experiments which were performed with different amounts of pDNA and different treatment modalities. In neither one of them, hPTCH1-wt promoter was induced significantly upon treatment with shh protein (1µg/ml):

Graph A shows a Hedgehog experiment in which, 400ng of hPTCH1-wt and 400ng of mutated hPTCHMut were transfected per well in NIH 3T3 cells. Treatment with shh protein was performedaccording to treatment 1. Regarding the functional promoter hPTCH1-wt, cells treated with shh produced a higher light signal (11.9 RLU) compared to cells which received loading control co(shh) (3.0 RLU). Due to high sample to sample variability, signal increase was not statistically significant in hPTCH1-wt. By contrast, the mutated version hPTCHMut was not induced upon shh treatment. However, light intensity of hPTCHMut (27.6-38.8 RLU) was higher than light intensity of hPTCH1-wt (3.0-11.9 RLU). The mutated version of a promoter should have lower transcriptional activity than the functional promoter.
Graph B shows the results of a Hedgehog experiment in which 200ng hPTCH1-wt and 200ng hPTCHMut were transfected per well in NIH 3T3 cells. Treatment with shh protein was performed according to treatment 2. In this experiment, light intensity of cells transfected with hPTCH1-wt and hPTCHMut, regardless of whether treated with shh protein or loading control, was comparable (51.3-57.1 RLU). Both functional and mutated promoter were not inducible upon treatment with Hedgehog activator.

To conclude, hPTCH1-wt promoter was not significantly inducible upon treatment with shh protein. In addition, the mutated version hPTCHMut produced a high baseline signal similar to that of the functional promoter. Our results were not reproducible.

4.4.2 No difference in Hedgehog activation with different treatment modalities

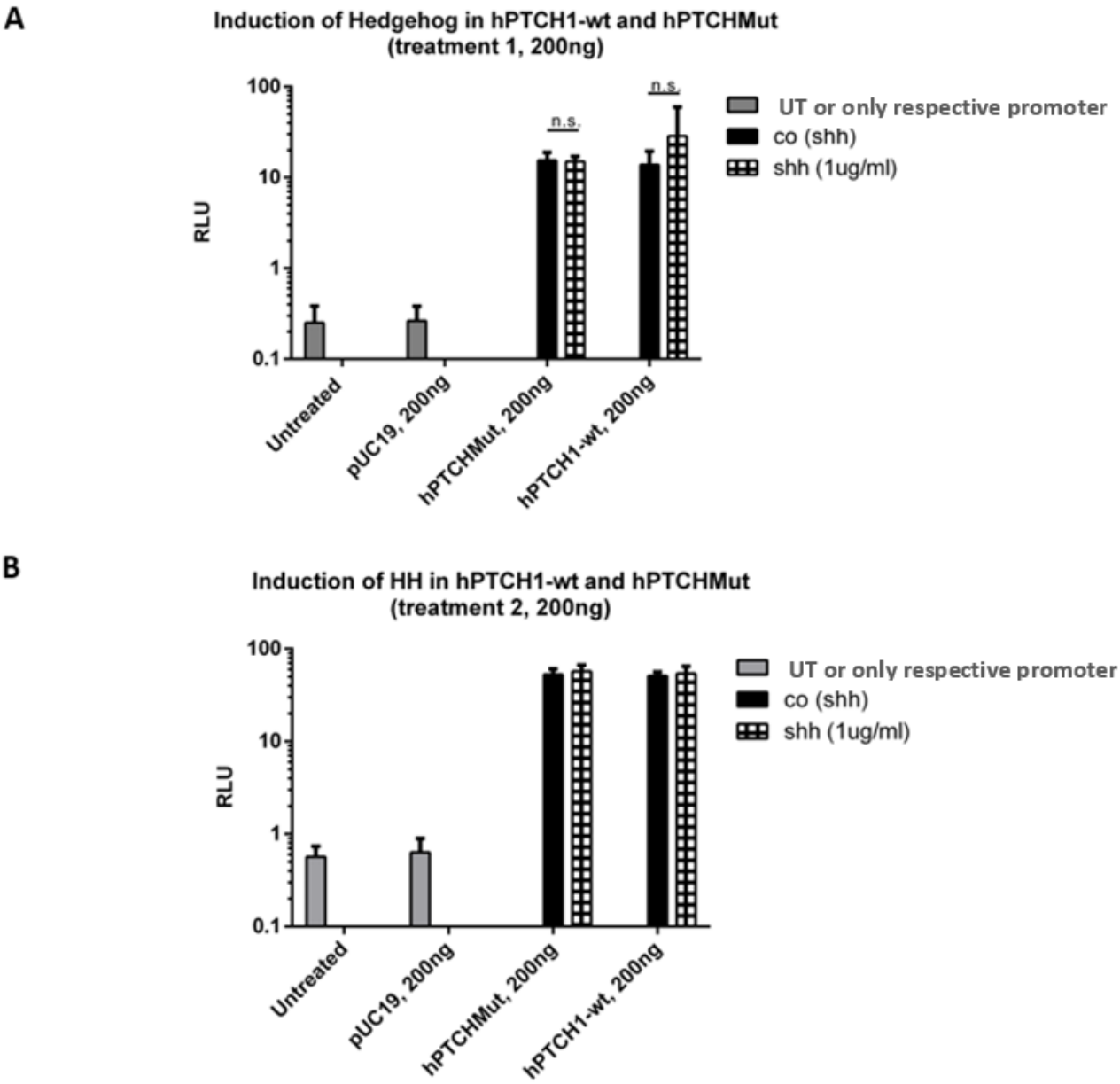

Figure 22. Activation of Hedgehog in hPTCH1-wt and hPTCHMut in NIH 3T3 cell line A) Normalized Fluc values of all conditions (untreated cells, pUC19, hPTCHMut, hPTCH1-wt, 200ng each). Cells received shh protein (1µg/ml) according to treatment 1: 4h after transfection, medium was aspirated and 50µl shh was added per well B) Normalized Fluc values of all conditions (untreated cells, pUC19, hPTCHMut, hPTCH1-wt, 200ng each). Cells received shh protein (1µg/ml) according to treatment 2: 4h after transfection, 100µl shh was added per well. Hedgehog activation was compared to cells which were treated with loading control co(shh).

From in total five Hedgehog experiments, in three experiments cells were treated according to treatment 1 (50µl/ well) and in two experiments according to treatment 2 (200µl/ well). In KP15 and KP18 (treatment 1)), signal increase was measureable in functional promoter hPTCH1-wt after treatment with shh protein (1µg/ml). These two experiments were performed with two different treatment modalities but the same amount of pDNA. In the other three experiments (KP14, KP19, KP20), no signal increase was measured in cells transfected with hPTCH1-wt upon activator treatment (treatment 1 and treatment 2).

Graph A shows experiment KP18 (treatment 1. 200ng): Upon treatment with shh protein, hPTCH1-wt produced a higher light intensity (28.7 RLU) compared to cells treated with loading control (13.9 RLU). Again, signal increase of RLU was not statistically significant.

Graph B shows experiment KP19 (treatment 2. 200ng): In cells transfected with hPTCH1-wt light signal is comparable (51.3-54.3 RLU), regardless of whether treated with shh or loading control co(shh).

To conclude, two different treatment modalities of Hedgehog activator shh led to similar results regarding activation of Hedgehog in fuctional Hedgehog promoter hPTCH1-wt.

5 Discussion

5.1 Assumptions why 3P-TOP was partly inducible

Visualisation of Wnt, Notch and Hedgehog activity in our reporter construct 3P-TOP was only successful in regard to Notch signalling pathway. Notch was the only pathway inducible trough co-transfection of murine Notch activator pCAGGS-NICD. Concerning Wnt and Hedgehog pathways, measured fluorescence emission of fluorescent proteins was comparable in cells treated with pathway-specific activators and in cells treated with loading control. Hence, these two developmental pathways could not be specifically activated in 3P-TOP. For this reason, we decided to assess promoter activity in luminescence assay instead of fluorescence assay: Wnt-dependent promoter TOPFlash was highly inducible upon treatment with wnt3A. By contrast, hPTCH1-wt promoter showed no significant increase in promoter activity upon sonic hedgehog (shh) treatment. As such, our results of Hedgehog experiments were not consistent.
The question remains why all three pathways could not be activated simultaneously in fluorescence assay. In the following section some possible explanations are listed:

- Our reporter construct 3P-TOP is a huge plasmid (almost 15kB) as it contains a lentiviral backbone. Due to negative correlation of plasmid size and transfection efficiency, the size of our reporter construct could aggravate cell uptake and gene expression of pathway-dependent promoters.
- Expression of fluorescent proteins is dependent on promoter activity: e.g. if CBF (Notch) is a stronger promoter than TOPFlash (Wnt), transcriptional activity of its downstream fluorophore tdTomato will be higher and, as such, fluorescence signal of tdTomato will be higher than iRFP signal.
- EGFP is one of the brightest and most photostable fluorescent proteins (Day und Davidson 2009). Fused to constitutive active CMV promoter in 3P-TOP, EGFP expression in cells is higher than that of other fluorescent proteins. This fact could explain its interference into channels of other fluorescence proteins albeit signal of each fluorescent protein was compensated in course of evaluation. EGFP may overlap signal of other fluorescent proteins and thus pathway activity may appear less than it is.
- Different assessment of pathway activators: Notch pathway was activated due to co-transfection of Notch promoter and murine Notch activator. On the contrary, Wnt and Hedgehog dependent promoters were induced with recombinant proteins. Transient transfection of pathway activators could possibly be more efficient than post-transfectional treatment with proteins.
- Cell line, timepoints of treatment and read-out were not adequate for our reporter construct
- In the worst case, something went wrong in the process of reporter plasmid construction

We assume that our reporter construct 3P-TOP would perform better if luciferases were used as reporter genes instead of fluorescent proteins. Firefly luciferase is commonly used in reporter gene assays due to its high sensitivity and broad linear range up to 7-8 orders of magnitude (Naylor 1999).

As fluorescent proteins lack enzymatic amplification, they are less sensitive compared to luciferases which makes them inferior to quantitative measurement of gene expression (Naylor 1999). For this reason, a new reporter construct will be generated containing luciferases as reporter genes to visualize pathway activity.

5.2 Venus is a brighter fluorescent protein than tdTomato

In our Notch experiments, cbf-tdTomato was compared to cbf-H2B-Venus. The purpose was to investigate if the fluorescent protein itself has an impact on the results as transcriptional activity of fluorescent genes fused to the same promoter (CBF) should be the same. In the process of evaluation, cells transfected with Venus emitted a higher and brighter fluorescence signal compared to cells transfected with tdTomato.

Venus belongs to Yellow fluorescent proteins (YFP) which are derivatives of green fluorescent protein (GFP). For this reason, Venus emits light in a similar range as EGFP with a shift in yellow spectrum. It was developed to have increased brightness (52.55) compared to EGFP (33.6). In addition, Venus has a long fluorescence life-time of 3.0 ns (table 8).

tdTomato is one of the brightest red fluorescent proteins (95.22) due to its tandem dimer structure which manifests in its high molecular weight (54.2 kDa). Although tdTomato is one of the brightest fluorescent proteins, in our experiments it appeared to produce a smaller fluorescence signal in contrast to Venus. One possible explanation for this could be that Venus emits fluorescence signal in the channels allocated to tdTomato, namely B2-A and B3-A. As compensation matrix was generated, only four channels were chosen to be compesated for spectral overlap (comp. V2-A, comp. B1-A, comp. B3-A and comp. R2-A); see table 5 and 6. However, tdTomato emits mostly in B2-A and B3-A channels. As only B3-A channel was compensated, tdTomato signal was evaluated with comp. B3-A/ comp. R2-A. Thus, tdTomato signal in B2-A channel is not available for evaluation of tdTomato signal if compensation is used.

Another reason for low tdTomato signal compared to Venus could be a reduced half-life of tdTomato protein in the cells. During research for this thesis, no data regarding protein half-life of Venus or tdTomato could be found. However, shorter half-life of tdTomato could be a possible explanation for lower fluorescence signal compared to Venus.

Commonly, fluorescent proteins have a protein half-life-time of 24 hours (Snapp 2009). High protein stability may however limit application of fluorescence proteins in studies which require high turnover rates, e.g. transcriptional induction studies (Li et al. 1998). Rapid turnover is related to protein degradation which can be induced through signals e.g. PEST signals, phosphorylation or protein-protein interaction (Li et al. 1998). Li et al concluded that fluorescence decay correlates with protein degradation. Thus, rapid turnover is linked to shorter half-life of proteins.

Name	Excitation	Emission	EC	QY	Brighness	Bleaching	Maturation	MW
mT2	434 nm	474 nm	30.000	0.93	27.9	90 s	/	26.9 kDa
EGFP	488 nm	507 nm	56.000	0.6	33.6	174 s	25 min	26.9 kDa
Venus	515 nm	528 nm	92.000	0.57	52.5	15 s	/	26.8 kDa
tdTomato	554 nm	581 nm	138.000	0.69	95.2	70 s	60 min	54.2 kDa
iRFP	690 nm	713 nm	105.000	0.06	6.3	450 s	168 min	34.6 kDa

Table 8. Spectral and biochemical properties of fluorescent proteins: abbreviations and definitions: Maximum excitation and maximum emission wavelenghts from fluorescent proteins (nm); EC=extinction coefficient of fluorescent proteins ($M^{-1} cm^{-1}$); QY= Quantum yield is the ratio of emitted photons to absorbed photons and determines efficiency of a fluorescent protein to emit photons (www.sciencedirect.com);Brightness is the product of quantum yield and extinction coefficient and determines how bright a fluorescent protein is (Snapp 2009); Maturation is the time needed for correct folding of a fluorescent protein (min) (Snapp 2009); Bleaching refers to photostability defining time of possible excitation of a fluorescent protein before photobleaching occurs (s) (Snapp 2009). (Data from FPbase)

5.3 Importance of compensation in multi-colour experiments

Fluorescence compensation is needed for simultaneous detection of multiple fluorescent proteins, especially if four fluorescent proteins genes are combined in one reporter construct, as it is in our case. During establishment of a compensation matrix, Julia Maier and Islam Abd-El Rahman noticed following facts in their experiments:

- EGFP gives a signal overspill in the tdTomato emission spectrum (Abd El Rahman 2017)
- EGFP gives a signal overspill in the mTurquoise2 emission spectrum (Abd El Rahman 2017)

In order to further investigate these findings, our 3P-TOP experiment was evaluated firstly, with compensation, and secondly, without. Here a brief overview of the results (4.5.2):

- Percentage of $EGFP^+$ cells was comparable (around 47%)
- Percentage of $tdTomato^+$ cells was comparable (in the range of 2-22%)
- Percentage of $iRFP^+$ cells was higher in compensated channels (26-29%) than in non-compensated channels (10-12%)
- Percentage of $mTurquoise2^+$ cells was lower in compensated channels (2-3%) than in non-compensated channels (16-18%)

Although percentage of $tdTomato^+$ cells was comparable, interplay of EGFP and tdTomato could be observed. EGFP gives a signal spillover in B2-A channel which is also used for detection of tdTomato signal besides B3-A channel. This can be explained by the broad emission spectrum of EGFP ($emission_{max}$ at 507nm) which partially overlaps with excitation and emission spectrum of tdTomato ($excitation_{max}$ at 554nm, $emission_{max}$ at 581nm), as depicted in figure 23. Consequently, EGFP enhances the fluorescence signal of tdTomato in B2-A channel.

For this reason, EGFP spillover in B2-A channel should be compensated and tdTomato thus evaluated in comp. B2-A/comp. B3-A instead of comp. B3-A/comp. R2-A.

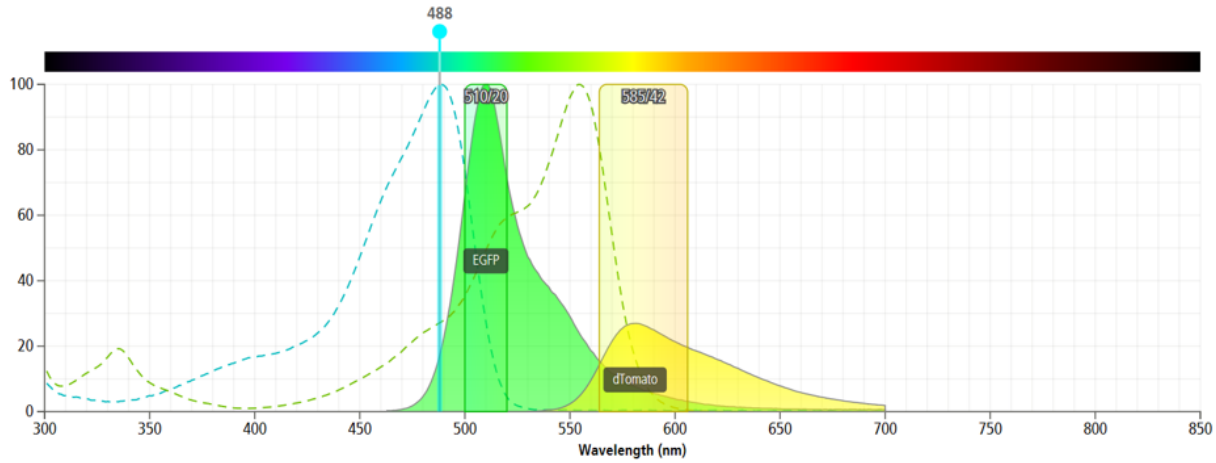

Figure 23. Spectral overlap of EGFP and tdTomato: Excitation maxima (dashed lines) and emission maxima (continuos lines) of EGFP (green) and tdTomato (yellow) are depicted. (Graph generated with "SpectrumViewer" provided by BD Biosciences)

Regarding mTurquoise2 signal, percentage of mTurquoise2$^+$ cells was lower in comp. V2-A channel than in non-compensated V2-A channel. As EGFP emits fluorescence maximally at 507nm, V2-A emission filter (525/ 50nm) detects fluorescence signal also in the range of EGFP emission. In this way, eGFP shines into V2-A channel used for detection of mTurquoise. EGFP spillover could eventually be minimized, if mTurquoise2 was excited with violet laser (405nm) instead of blue laser (488nm) and then evaluated with comp. V2-A/comp. B1-A.

The fact that EGFP fluorescence is also detected in channels assigned to mTurquoise2 and tdTomato underlines the necessity to use compensation in multi-colour experiments.

5.4 hPTCH1-wt promoter was not inducible

Although different amounts of promoter DNA and treatment modalities of Hedgehog activator were used, Hedgehog promoter hPTCH1-wt was not inducible upon treatment with sonic hedgehog protein. In addition, the mutated version hPTCHMut produced comparable luminescence signal to hPTCH1-wt indicating that hPTCHMut has a similar transcription to hPTCH1-wt. For this outcome the cell line used might not cause this effect, as NIH 3T3 cells are used in various papers for monitoring Hedgehog pathway activity (Rohatgi et al. 2007; Kim et al. 2009). In addition, BPS Bioscience promote NIH 3T3 as "Gli reporter cell line for monitoring Hedgehog signalling pathway activity" (http://bpsbioscience.com/hedgehog-pathway-gli-reporter-60409). For this reason, we assume that hPTCH1-wt promoter is not suitable for our purposes. Hedgehog activity could not be induced in hPTCH1-wt, neither in fluorescence assay nor in luminescence assay. According to our results, the mutated version hPTCHMut seemed to have the same transcriptional activity as the functional one.

In further experiments, a new Hedgehog promoter and new activator will be tested, namely 12xGLI-RETKO-Luc (Kogerman et al. 1999; Rahnama et al. 2006) and pLUT7 HA-GLI1 (Addgene plasmid # 62970) in NIH 3T3 cells. 12x GLI-RETKO-Luc contains 12 GLI-binding sites as a tandem repeat fused to thymidine kinase basic promoter (Rahnama et al. 2006) whereas pLUT7 HA-GLI1 expresses GLI 1 (transcriptional activator). If Hedgehog activation can be achieved, the new Hedgehog promoter will be used in a new reporter construct.

6 Appendix

6.1 Abstract

Cancer is still one of major death causes worldwide. Developmental signalling pathways such as Wnt, Notch and Hedgehog, usually involved in tissue homeostasis and embryonic development, are found to be deregulated in many types of cancer. Understanding how these pathways are coordinated, how they interplay and how they are altered in cancer provides more insight in the process of oncogenesis and subsequently the possibility for development of new and highly specific treatment strategies of cancer.

The major topic of this thesis was to assess function of our reporter construct 3P-TOP which dynamically visualizes activity of Wnt, Notch and Hedgehog pathways. The reporter construct comprises three pathway-dependent promoters (CBF, TOPFlash, hPTCH1) driving the expression of distinct fluorescent proteins (tdTomato, iRFP, mTurquoise2). In addition, constitutive active CMV promoter drives expression of EGFP which is therefore always expressed providing information about transfection efficiency. Our reporter construct was transfected into lung cancer cell line A549 and promoters were induced upon addition of pathway specific activators. Increase in fluorescence signal and thus pathway activity was measured via flow cytometry. However, in fluorescence assay only activation of Notch pathway could be achieved. Hence, all three pathway-dependent promoters (CBF, TOPFlash, hPTCH1) were tested separately for their inducibility in fluorescence assay (CBF) and bioluminescence assay (TOPFlash and hPTCH1). Bioluminescence assay was performed due to higher sensitivity and enzymatic amplification of Firefly luciferase compared to fluorescent proteins. Finally, our results revealed that Wnt and Notch dependent promoters (CBF and TOPFlash) could be induced upon activator treatment while testing of Hedgehog dependent promoter (hPTCH1) showed no reproducible results. In future experiments, a new reporter construct will be generated containing a different Hedgehog promoter and luciferases reporter genes instead of fluorescent proteins.

Reporter gene constructs offer the opportunity to study function of e.g. pathway-specific promoters from certain signalling pathways often deregulated in cancer. With this knowledge, new treatment approaches can be developed providing cancer patients higher survival chances and lower relapse rate.

6.2 Zusammenfassung

Krebs ist weiterhin eine der Haupttodesursachen weltweit. Signaltransduktionswege wie z.B. Wnt, Notch und Hedgehog, welche normalerweise an Gewebshomöostase und in der Embryonalentwicklung beteiligt sind, sind oftmals in vielen Arten von Krebs dereguliert. Das Verständnis darüber wie diese Signaltransduktionswege koordiniert sind, wie sie miteinander wechselwirken und inwiefern sie in Krebs dereguliert sind, bietet uns einen größeren Einblick in die Karzinogenese und die Möglichkeit, neue, hoch-spezifische Behandlungsstrategien gegen Krebs zu entwickeln.

Eines der Hauptziele dieser Arbeit war, die Funktion des Reporterkonstrukts 3P-TOP zu testen, welches die Aktivität der drei oben genannten Signaltransduktionswege dynamisch visualisieren soll. Das Reporterkonstrukt besteht aus drei Promotoren (CBF, TOPFlash, hPTCH1), welche Signaltransduktionsweg-abhängig aktiviert werden, und aus Genen welche für Fluorophore kodieren. Zusätzlich enthalten ist ein konstitutiv aktiver Promotor (CMV), der die Expression von EGF vorantreibt, welches daher immer exprimiert wird und Aufschluss über die Transfektionseffizienz bietet. Unser Reporterkonstrukt wurde in die Lungenkarzinom-Zelllinie A549 transfiziert und durch Zugabe von Signaltransduktions-abhängigen Aktivatoren induziert. Eine Erhöhung des Fluoreszenzsignals, welches mit der Aktivierung eines Signaltransduktionsweges korreliert, wurde mittels Durchflusszytometrie vermessen. Allerdings konnte im Fluoreszenzassay nur der Notch Signaltransduktionsweg aktiviert werden. Aus diesem Grund wurden alle drei Signaltransduktionsweg-abhängigen Promotoren (CBF, TOPFlash, hPTCH1) separat auf ihre Induzierbarkeit in zwei verschiedenen Assays getestet: im Fluoreszenzassay (CBF) und im Biolumineszenzassay (TOPFlash, hPTCH1). Der Biolumineszenzassay wurde aufgrund der höheren Sensitivität und enzymbedingten Signalamplifizierung der Glühwürmchen-Luciferase im Vergleich zu Fluoreszenzproteinen durchgeführt. Schlussendlich ergaben unsere Ergebnisse, dass die Wnt und Notch-abhängigen Promotoren (TOPFlash, CBF) mittels Zugabe von Aktivatoren induziert werden konnten. Im Vergleich dazu konnte der Hedgehog-abhängige Promotor (hPTCH1) nicht induziert werden und lieferte keine reproduzierbaren Ergebnisse. In zukünftigen Experimenten wird ein neues Reporterkonstrukt gebaut werden, dass einen anderen Hedgehog-abhängigen Promotor enthalten wird und Luciferasen als Reportergene anstelle von Fluoreszenzproteinen.

Reportergenkonstrukte bieten die Möglichkeit, die Funktion von Promotoren zu testen wie z.B. Promotoren bestimmter Signaltransduktionswege, die in Krebs oftmals dereguliert sind. Mit diesem Wissen können neue Therapiestrategien gegen Krebs entwickelt werden, welche Krebspatienten eine höhere Überlebenschance und eine geringere Rückfallquote bieten könnten.

7 References

Abd El Rahman, Islam (2017): Evaluation of multi-colour transfections via flow cytometry. Vienna, University of Vienna, diploma thesis. University of Vienna, Vienna.

Al-Hajj, Muhammad; Wicha, Max S.; Benito-Hernandez, Adalberto; Morrison, Sean J.; Clarke, Michael F. (2003): Prospective identification of tumorigenic breast cancer cells. In: *Proceedings of the National Academy of Sciences of the United States of America* 100 (7), S. 3983–3988. DOI: 10.1073/pnas.0530291100.

Athar, Mohammad; Tang, Xiuwei; Lee, Juliette L.; Kopelovich, Levy; Kim, Arianna L. (2006): Hedgehog signalling in skin development and cancer. In: *Experimental dermatology* 15 (9), S. 667–677. DOI: 10.1111/j.1600-0625.2006.00473.x.

Badr, Christian E.; Tannous, Bakhos A. (2011): Bioluminescence imaging: progress and applications. In: *Trends in biotechnology* 29 (12), S. 624–633. DOI: 10.1016/j.tibtech.2011.06.010.

Baumgarth, Nicole; Roederer, Mario (2000): A practical approach to multicolor flow cytometry for immunophenotyping. In: *Journal of Immunological Methods* 243 (1-2), S. 77–97. DOI: 10.1016/S0022-1759(00)00229-5.

Beck, Benjamin; Blanpain, Cédric (2013): Unravelling cancer stem cell potential. In: *Nature reviews. Cancer* 13 (10), S. 727–738. DOI: 10.1038/nrc3597.

Boeckle, Sabine; Gersdorff, Katharina von; van der Piepen, Silke; Culmsee, Carsten; Wagner, Ernst; Ogris, Manfred (2004): Purification of polyethylenimine polyplexes highlights the role of free polycations in gene transfer. In: *The journal of gene medicine* 6 (10), S. 1102–1111. DOI: 10.1002/jgm.598.

Boussif, O.; Lezoualc'h, F.; Zanta, M. A.; Mergny, M. D.; Scherman, D.; Demeneix, B.; Behr, J. P. (1995a): A versatile vector for gene and oligonucleotide transfer into cells in culture and in vivo: polyethylenimine. In: *Proceedings of the National Academy of Sciences of the United States of America* 92 (16), S. 7297–7301.

Boussif, O.; Lezoualc'h, F.; Zanta, M. A.; Mergny, M. D.; Scherman, D.; Demeneix, B.; Behr, J. P. (1995b): A versatile vector for gene and oligonucleotide transfer into cells in culture and in vivo: polyethylenimine. In: *Proceedings of the National Academy of Sciences of the United States of America* 92 (16), S. 7297–7301. DOI: 10.1073/pnas.92.16.7297.

Campbell, Robert E.; Tour, Oded; Palmer, Amy E.; Steinbach, Paul A.; Baird, Geoffrey S.; Zacharias, David A.; Tsien, Roger Y. (2002): A monomeric red fluorescent protein. In: *Proceedings of the National Academy of Sciences of the United States of America* 99 (12), S. 7877–7882. DOI: 10.1073/pnas.082243699.

Cengizeroglu, Arzu (2012): Targeted RNAi and pDNA based therapy for gastrointestinal tumors. München, Ludwig-Maximilians-Universität, Diss., 2012. Universitätsbibliothek der Ludwig-Maximilians-Universität, München.

Chen, Ke; Huang, Ying-hui; Chen, Ji-long (2013): Understanding and targeting cancer stem cells: therapeutic implications and challenges. In: *Acta pharmacologica Sinica* 34 (6), S. 732–740. DOI: 10.1038/aps.2013.27.

Chira, Sergiu; Jackson, Carlo S.; Oprea, Iulian; Ozturk, Ferhat; Pepper, Michael S.; Diaconu, Iulia et al. (2015): Progresses towards safe and efficient gene therapy vectors. In: *Oncotarget* 6 (31), S. 30675–30703. DOI: 10.18632/oncotarget.5169.

Choosakoonkriang, Sirirat; Lobo, Brian A.; Koe, Gary S.; Koe, Janet G.; Middaugh, C. Russell (2003): Biophysical characterization of PEI/DNA complexes. In: *Journal of pharmaceutical sciences* 92 (8), S. 1710–1722. DOI: 10.1002/jps.10437.

Choy, Garry; Choyke, Peter; Libutti, Steven K. (2003): Current Advances in Molecular Imaging: Noninvasive in Vivo Bioluminescent and Fluorescent Optical Imaging in Cancer Research. In: *Mol Imaging* 2 (4), 153535002003031. DOI: 10.1162/15353500200303142.

Chtarbova, Slava; Nimmrich, Inko; Erdmann, Silke; Herter, Peter; Renner, Matthias; Kitajewski, Jan; Müller, Oliver (2002): Murine Nr4a1 and Herpud1 are up-regulated by Wnt-1. but the homologous human genes are independent from beta-catenin activation. In: *The Biochemical journal* 367 (Pt 3), S. 723–728. DOI: 10.1042/bj20020699.

Clevers, Hans (2011): The cancer stem cell: premises, promises and challenges. In: *Nature medicine* 17 (3), S. 313–319. DOI: 10.1038/nm.2304.

da Costa, L. T.; He, T. C.; Yu, J.; Sparks, A. B.; Morin, P. J.; Polyak, K. et al. (1999): CDX2 is mutated in a colorectal cancer with normal APC/beta-catenin signaling. In: *Oncogene* 18 (35), S. 5010–5014. DOI: 10.1038/sj.onc.1202872.

Daunert, Sylvia; Deo, Sapna K. (2006): Photoproteins in bioanalysis. Weinheim: Wiley-VCH. Online verfügbar unter http://site.ebrary.com/lib/alltitles/docDetail.action?docID=10303930.

Day, Richard N.; Davidson, Michael W. (2009): The fluorescent protein palette: tools for cellular imaging. In: *Chemical Society reviews* 38 (10), S. 2887–2921. DOI: 10.1039/b901966a.

Di Gioia, Sante; Conese, Massimo (2009): Polyethylenimine-mediated gene delivery to the lung and therapeutic applications. In: *Drug design, development and therapy* 2. S. 163–188.

Dick, John E. (2008): Stem cell concepts renew cancer research. In: *Blood* 112 (13), S. 4793–4807. DOI: 10.1182/blood-2008-08-077941.

Espinoza, Ingrid; Miele, Lucio (2013): Notch inhibitors for cancer treatment. In: *Pharmacology & therapeutics* 139 (2), S. 95–110. DOI: 10.1016/j.pharmthera.2013.02.003.

Espinoza, Ingrid; Pochampally, Radhika; Xing, Fei; Watabe, Kounosuke; Miele, Lucio (2013): Notch signaling: targeting cancer stem cells and epithelial-to-mesenchymal transition. In: *OncoTargets and therapy* 6. S. 1249–1259. DOI: 10.2147/OTT.S36162.

Filonov, Grigory S.; Piatkevich, Kiryl D.; Ting, Li-Min; Zhang, Jinghang; Kim, Kami; Verkhusha, Vladislav V. (2011): Bright and stable near-infrared fluorescent protein for in vivo imaging. In: *Nature biotechnology* 29 (8), S. 757–761. DOI: 10.1038/nbt.1918.

Funhoff, Arjen M.; van Nostrum, Cornelus F.; Koning, Gerben A.; Schuurmans-Nieuwenbroek, Nancy M. E.; Crommelin, Daan J. A.; Hennink, Wim E. (2004): Endosomal escape of polymeric gene delivery complexes is not always enhanced by polymers buffering at low pH. In: *Biomacromolecules* 5 (1), S. 32–39. DOI: 10.1021/bm034041.

Gaedtke, Lars; Pelisek, Jaroslav; Lipinski, Kai S.; Wrighton, Christopher J.; Wagner, Ernst (2007): Transcriptionally targeted nonviral gene transfer using a beta-catenin/TCF-dependent promoter

in a series of different human low passage colon cancer cells. In: *Molecular pharmaceutics* 4 (1), S. 129–139. DOI: 10.1021/mp0600586.

Goedhart, Joachim; Stetten, David von; Noirclerc-Savoye, Marjolaine; Lelimousin, Mickaël; Joosen, Linda; Hink, Mark A. et al. (2012): Structure-guided evolution of cyan fluorescent proteins towards a quantum yield of 93%. In: *Nature communications* 3. S. 751. DOI: 10.1038/ncomms1738.

Grandinetti, Giovanna; Ingle, Nilesh P.; Reineke, Theresa M. (2011): Interaction of poly(ethylenimine)-DNA polyplexes with mitochondria: implications for a mechanism of cytotoxicity. In: *Molecular pharmaceutics* 8 (5), S. 1709–1719. DOI: 10.1021/mp200078n.

Greer, Lee F.; Szalay, Aladar A. (2002): Imaging of light emission from the expression of luciferases in living cells and organisms: a review. In: *Luminescence : the journal of biological and chemical luminescence* 17 (1), S. 43–74. DOI: 10.1002/bio.676.

Hanahan, Douglas; Weinberg, Robert A. (2000): The Hallmarks of Cancer. In: *Cell* 100 (1), S. 57–70. DOI: 10.1016/S0092-8674(00)81683-9.

Hanahan, Douglas; Weinberg, Robert A. (2011): Hallmarks of cancer: the next generation. In: *Cell* 144 (5), S. 646–674. DOI: 10.1016/j.cell.2011.02.013.

Hawley, Teresa S.; Herbert, Donald J.; Eaker, Shannon S.; Hawley, Robert G. (2004): Multiparameter flow cytometry of fluorescent protein reporters. In: *Methods in molecular biology (Clifton, N.J.)* 263. S. 219–238. DOI: 10.1385/1-59259-773-4:219.

Jin, Lian; Zeng, Xin; Liu, Ming; Deng, Yan; He, Nongyue (2014): Current progress in gene delivery technology based on chemical methods and nano-carriers. In: *Theranostics* 4 (3), S. 240–255. DOI: 10.7150/thno.6914.

Karamboulas, Christina; Ailles, Laurie (2013): Developmental signaling pathways in cancer stem cells of solid tumors. In: *Biochimica et Biophysica Acta (BBA) - General Subjects* 1830 (2), S. 2481–2495. DOI: 10.1016/j.bbagen.2012.11.008.

Kawakami, Shigeru; Ito, Yoshitaka; Charoensit, Pensri; Yamashita, Fumiyoshi; Hashida, Mitsuru (2006): Evaluation of proinflammatory cytokine production induced by linear and branched polyethylenimine/plasmid DNA complexes in mice. In: *The Journal of pharmacology and experimental therapeutics* 317 (3), S. 1382–1390. DOI: 10.1124/jpet.105.100669.

Kircheis, Ralf; Wagner, Ernst (2000): Polycation/DNA complexes for in vivo gene delivery. In: *Gene Therapy and Regulation* 1 (1), S. 95–114. DOI: 10.1163/156855800744557.

Kogerman, P.; Grimm, T.; Kogerman, L.; Krause, D.; Undén, A. B.; Sandstedt, B. et al. (1999): Mammalian suppressor-of-fused modulates nuclear-cytoplasmic shuttling of Gli-1. In: *Nature cell biology* 1 (5), S. 312–319. DOI: 10.1038/13031.

Korinek, V. (1997): Constitutive Transcriptional Activation by a beta -Catenin-Tcf Complex in APC-/- Colon Carcinoma. In: *Science* 275 (5307), S. 1784–1787. DOI: 10.1126/science.275.5307.1784.

Kreso, Antonija; Dick, John E. (2014): Evolution of the Cancer Stem Cell Model. In: *Cell Stem Cell* 14 (3), S. 275–291. DOI: 10.1016/j.stem.2014.02.006.

Lecoq, Jérôme; Schnitzer, Mark J. (2011): An infrared fluorescent protein for deeper imaging. In: *Nature biotechnology* 29 (8), S. 715–716. DOI: 10.1038/nbt.1941.

Li, Xianqiang; Zhao, Xiaoning; Fang, Yu; Jiang, Xin; Duong, Tommy; Fan, Connie et al. (1998): Generation of Destabilized Green Fluorescent Protein as a Transcription Reporter. In: *J. Biol. Chem.* 273 (52), S. 34970–34975. DOI: 10.1074/jbc.273.52.34970.

Lipinski, Kai S.; Djeha, Hakim A.; Gawn, Jonathan; Cliffe, Suzanne; Maitland, Norman J.; Palmer, Daniel H. et al. (2004): Optimization of a synthetic beta-catenin-dependent promoter for tumor-specific cancer gene therapy. In: *Molecular therapy : the journal of the American Society of Gene Therapy* 10 (1), S. 150–161. DOI: 10.1016/j.ymthe.2004.03.021.

MacDonald, Bryan T.; He, Xi (2012): Frizzled and LRP5/6 receptors for Wnt/β-catenin signaling. In: *Cold Spring Harbor perspectives in biology* 4 (12). DOI: 10.1101/cshperspect.a007880.

Miyata, Kanjiro; Nishiyama, Nobuhiro; Kataoka, Kazunori (2012): Rational design of smart supramolecular assemblies for gene delivery: chemical challenges in the creation of artificial viruses. In: *Chemical Society reviews* 41 (7), S. 2562–2574. DOI: 10.1039/c1cs15258k.

Mizutani, Ken-ichi; Yoon, Keejung; Dang, Louis; Tokunaga, Akinori; Gaiano, Nicholas (2007): Differential Notch signalling distinguishes neural stem cells from intermediate progenitors. In: *Nature* 449 (7160), S. 351–355. DOI: 10.1038/nature06090.

Moghimi, S. Moein; Symonds, Peter; Murray, J. Clifford; Hunter, A. Christy; Debska, Grazyna; Szewczyk, Adam (2005): A two-stage poly(ethylenimine)-mediated cytotoxicity: implications for gene transfer/therapy. In: *Molecular therapy : the journal of the American Society of Gene Therapy* 11 (6), S. 990–995. DOI: 10.1016/j.ymthe.2005.02.010.

Müller, Katharina Thekla (2017): Luciferase based reporter gene assays for investigating nucleic acid delivery *in vitro*. Vienna, University of Vienna, diploma thesis. University of Vienna, Vienna.

Müller, M. Ogris, H. Sami: Firefly luciferase based reporter gene assay for investigating nanoparticle mediated nucleic acid delivery , Chapter in Methods Mol Biol. 2019, in press

Nagai, Takeharu; Ibata, Keiji; Park, Eun Sun; Kubota, Mie; Mikoshiba, Katsuhiko; Miyawaki, Atsushi (2002): A variant of yellow fluorescent protein with fast and efficient maturation for cell-biological applications. In: *Nature biotechnology* 20 (1), S. 87–90. DOI: 10.1038/nbt0102-87.

Nakajima, Yoshihiro; Ohmiya, Yoshihiro (2010): Bioluminescence assays: multicolor luciferase assay, secreted luciferase assay and imaging luciferase assay. In: *Expert opinion on drug discovery* 5 (9), S. 835–849. DOI: 10.1517/17460441.2010.506213.

Naylor, Louise H. (1999): Reporter gene technology: the future looks bright. In: *Biochemical Pharmacology* 58 (5), S. 749–757. DOI: 10.1016/S0006-2952(99)00096-9.

Neu, Michael; Fischer, Dagmar; Kissel, Thomas (2005): Recent advances in rational gene transfer vector design based on poly(ethylene imine) and its derivatives. In: *The journal of gene medicine* 7 (8), S. 992–1009. DOI: 10.1002/jgm.773.

Ng, Jessica M. Y.; Curran, Tom (2011): The Hedgehog's tale: developing strategies for targeting cancer. In: *Nature reviews. Cancer* 11 (7), S. 493–501. DOI: 10.1038/nrc3079.

Nguyen, Long V.; Vanner, Robert; Dirks, Peter; Eaves, Connie J. (2012): Cancer stem cells: an evolving concept. In: *Nature reviews. Cancer* 12 (2), S. 133–143. DOI: 10.1038/nrc3184.

Nickoloff, B. J.; Qin, J-Z; Chaturvedi, V.; Denning, M. F.; Bonish, B.; Miele, L. (2002): Jagged-1 mediated activation of notch signaling induces complete maturation of human keratinocytes through NF-kappaB and PPARgamma. In: *Cell death and differentiation* 9 (8), S. 842–855. DOI: 10.1038/sj.cdd.4401036.

Niidome, T.; Huang, L. (2002): Gene therapy progress and prospects: nonviral vectors. In: *Gene therapy* 9 (24), S. 1647–1652. DOI: 10.1038/sj.gt.3301923.

Nowotschin, Sonja; Xenopoulos, Panagiotis; Schrode, Nadine; Hadjantonakis, Anna-Katerina (2013): A bright single-cell resolution live imaging reporter of Notch signaling in the mouse. In: *BMC developmental biology* 13. S. 15. DOI: 10.1186/1471-213X-13-15.

Ogris, M.; Steinlein, P.; Kursa, M.; Mechtler, K.; Kircheis, R.; Wagner, E. (1998): The size of DNA/transferrin-PEI complexes is an important factor for gene expression in cultured cells. In: *Gene therapy* 5 (10), S. 1425–1433. DOI: 10.1038/sj.gt.3300745.

Rahnama, Fahimeh; Shimokawa, Takashi; Lauth, Matthias; Finta, Csaba; Kogerman, Priit; Teglund, Stephan et al. (2006): Inhibition of GLI1 gene activation by Patched1. In: *The Biochemical journal* 394 (Pt 1), S. 19–26. DOI: 10.1042/BJ20050941.

Rémy-Kristensen, Arlette; Clamme, Jean-Pierre; Vuilleumier, Constance; Kuhry, Jean-Georges; Mély, Yves (2001): Role of endocytosis in the transfection of L929 fibroblasts by polyethylenimine/DNA complexes. In: *Biochimica et Biophysica Acta (BBA) - Biomembranes* 1514 (1), S. 21–32. DOI: 10.1016/S0005-2736(01)00359-5.

Reya, Tannishtha; Morrison, Sean J.; Clarke, Michael F.; Weissman, Irving L. (2001): Stem cells, cancer, and cancer stem cells. In: *Nature* 414 (6859), S. 105–111. DOI: 10.1038/35102167.

Roda, Aldo; Guardigli, Massimo; Michelini, Elisa; Mirasoli, Mara (2009): Bioluminescence in analytical chemistry and in vivo imaging. In: *TrAC Trends in Analytical Chemistry* 28 (3), S. 307–322. DOI: 10.1016/j.trac.2008.11.015.

Rödl, Wolfgang; Schaffert, David; Wagner, Ernst; Ogris, Manfred (2013): Synthesis of polyethylenimine-based nanocarriers for systemic tumor targeting of nucleic acids. In: *Methods in molecular biology (Clifton, N.J.)* 948. S. 105–120. DOI: 10.1007/978-1-62703-140-0_8.

Shaner, Nathan C.; Campbell, Robert E.; Steinbach, Paul A.; Giepmans, Ben N. G.; Palmer, Amy E.; Tsien, Roger Y. (2004): Improved monomeric red, orange and yellow fluorescent proteins derived from Discosoma sp. red fluorescent protein. In: *Nature biotechnology* 22 (12), S. 1567–1572. DOI: 10.1038/nbt1037.

Shaner, Nathan C.; Steinbach, Paul A.; Tsien, Roger Y. (2005): A guide to choosing fluorescent proteins. In: *Nature methods* 2 (12), S. 905–909. DOI: 10.1038/nmeth819.

Snapp, Erik Lee (2009): Fluorescent proteins: a cell biologist's user guide. In: *Trends in Cell Biology* 19 (11), S. 649–655. DOI: 10.1016/j.tcb.2009.08.002.

Stambolic, Vuk; Ruel, Laurent; Woodgett, James R. (1996): Lithium inhibits glycogen synthase kinase-3 activity and mimics Wingless signalling in intact cells. In: *Current Biology* 6 (12), S. 1664–1669. DOI: 10.1016/S0960-9822(02)70790-2.

Taipale, Jussi; Beachy, Philip A. (2001): The Hedgehog and Wnt signalling pathways in cancer. In: *Nature* 411 (6835), S. 349–354. DOI: 10.1038/35077219.

Takebe, Naoko; Harris, Pamela J.; Warren, Ronald Q.; Ivy, S. Percy (2011): Targeting cancer stem cells by inhibiting Wnt, Notch and Hedgehog pathways. In: *Nature reviews. Clinical oncology* 8 (2), S. 97–106. DOI: 10.1038/nrclinonc.2010.196.

Takebe, Naoko; Miele, Lucio; Harris, Pamela Jo; Jeong, Woondong; Bando, Hideaki; Kahn, Michael et al. (2015): Targeting Notch, Hedgehog, and Wnt pathways in cancer stem cells: clinical update. In: *Nature reviews. Clinical oncology* 12 (8), S. 445–464. DOI: 10.1038/nrclinonc.2015.61.

Talcott, Bradford; Moore, Mary Shannon (1999): Getting across the nuclear pore complex. In: *Trends in Cell Biology* 9 (8), S. 312–318. DOI: 10.1016/S0962-8924(99)01608-6.

Tannous, Bakhos A.; Kim, Dong-Eog; Fernandez, Juliet L.; Weissleder, Ralph; Breakefield, Xandra O. (2005): Codon-optimized Gaussia luciferase cDNA for mammalian gene expression in culture and in vivo. In: *Molecular therapy : the journal of the American Society of Gene Therapy* 11 (3), S. 435–443. DOI: 10.1016/j.ymthe.2004.10.016.

Tian (2009): Role of Hedgehog signaling pathway in proliferation and invasiveness of hepatocellular carcinoma cells. In: *Int J Oncol* 34 (3). DOI: 10.3892/ijo_00000209.

Tirino, Virginia; Desiderio, Vincenzo; Paino, Francesca; Rosa, Alfredo de; Papaccio, Federica; La Noce, Marcella et al. (2013): Cancer stem cells in solid tumors: an overview and new approaches for their isolation and characterization. In: *FASEB journal : official publication of the Federation of American Societies for Experimental Biology* 27 (1), S. 13–24. DOI: 10.1096/fj.12-218222.

Tung, James W.; Parks, David R.; Moore, Wayne A.; Herzenberg, Leonard A.; Herzenberg, Leonore A. (2004): New approaches to fluorescence compensation and visualization of FACS data. In: *Clinical Immunology* 110 (3), S. 277–283. DOI: 10.1016/j.clim.2003.11.016.

Vu, Lucas; Ramos, James; Potta, Thrimoorthy; Rege, Kaushal (2012): Generation of a focused poly(amino ether) library: polymer-mediated transgene delivery and gold-nanorod based theranostic systems. In: *Theranostics* 2 (12), S. 1160–1173. DOI: 10.7150/thno.4492.

Ward, Ryan J.; Dirks, Peter B. (2007): Cancer stem cells: at the headwaters of tumor development. In: *Annual review of pathology* 2. S. 175–189. DOI: 10.1146/annurev.pathol.2.010506.091847.

Welsh, Stephen; Kay, Steve A. (1997): Reporter gene expression for monitoring gene transfer. In: *Current Opinion in Biotechnology* 8 (5), S. 617–622. DOI: 10.1016/S0958-1669(97)80038-9.

Wicking, Carol; Smyth, Ian; Bale, Allen (1999): The hedgehog signalling pathway in tumorigenesis and development. In: *Oncogene* 18 (55), S. 7844–7851. DOI: 10.1038/sj.onc.1203282.

Wightman, L.; Kircheis, R.; Rössler, V.; Carotta, S.; Ruzicka, R.; Kursa, M.; Wagner, E. (2001): Different behavior of branched and linear polyethylenimine for gene delivery in vitro and in vivo. In: *The journal of gene medicine* 3 (4), S. 362–372. DOI: 10.1002/jgm.187.

Willert, Karl; Nusse, Roel (2012): Wnt proteins. In: *Cold Spring Harbor perspectives in biology* 4 (9), a007864. DOI: 10.1101/cshperspect.a007864.

Winklmayr, Martina; Schmid, Carmen; Laner-Plamberger, Sandra; Kaser, Alexandra; Aberger, Fritz; Eichberger, Thomas; Frischauf, Anna-Maria (2010): Non-consensus GLI binding sites in

Hedgehog target gene regulation. In: *BMC molecular biology* 11. S. 2. DOI: 10.1186/1471-2199-11-2.

Wolff, Jon A.; Rozema, David B. (2008): Breaking the bonds: non-viral vectors become chemically dynamic. In: *Molecular therapy : the journal of the American Society of Gene Therapy* 16 (1), S. 8–15. DOI: 10.1038/sj.mt.6300326.

Youn, Hyewon; Chung, June-Key (2013): Reporter gene imaging. In: *AJR. American journal of roentgenology* 201 (2), W206-14. DOI: 10.2214/AJR.13.10555.

Zhang, Yuan; Satterlee, Andrew; Huang, Leaf (2012): In vivo gene delivery by nonviral vectors: overcoming hurdles? In: *Molecular therapy : the journal of the American Society of Gene Therapy* 20 (7), S. 1298–1304. DOI: 10.1038/mt.2012.79.